

This is a repository copy of *A competition-attenuation mechanism modulates thermoresponsive growth at warm temperatures in plants.*

White Rose Research Online URL for this paper:

<https://eprints.whiterose.ac.uk/189927/>

Version: Accepted Version

Article:

Li, Wei, Tian, Ying-Ying, Li, Jin Yu et al. (6 more authors) (2022) A competition-attenuation mechanism modulates thermoresponsive growth at warm temperatures in plants. *New Phytologist*. ISSN 1469-8137

<https://doi.org/10.1111/nph.18442>

Reuse

Items deposited in White Rose Research Online are protected by copyright, with all rights reserved unless indicated otherwise. They may be downloaded and/or printed for private study, or other acts as permitted by national copyright laws. The publisher or other rights holders may allow further reproduction and re-use of the full text version. This is indicated by the licence information on the White Rose Research Online record for the item.

Takedown

If you consider content in White Rose Research Online to be in breach of UK law, please notify us by emailing eprints@whiterose.ac.uk including the URL of the record and the reason for the withdrawal request.

1 **A competition-attenuation mechanism modulates thermoresponsive**
2 **growth at warm temperatures in Arabidopsis**

3 Wei Li^{1,2}, Ying-Ying Tian¹, Jin-Yu Li¹, Li Yuan³, Lin-Lin Zhang¹, Zhi-Ye Wang¹,
4 Xiaodong Xu³, Seth Jon Davis^{3,4} and Jian-Xiang Liu^{1,*}

5 ¹State Key Laboratory of Plant Physiology and Biochemistry, College of Life
6 Sciences, Zhejiang University, Hangzhou 310027, China.

7 ²College of Environmental and Resource Sciences, Zhejiang University,
8 Hangzhou 310027, China.

9 ³State Key Laboratory of Crop Stress Adaptation and Improvement, School of
10 Life Sciences, Henan University, Kaifeng 475004, China.

11 ⁴Department of Biology, University of York, Heslington, York, YO105DD, UK.

12

13 *Correspondence: jianxiangliu@zju.edu.cn

14

15 **Article type:**

16 Research article

17

18

19 **Short title:**

20 RVE5 regulates thermoresponsive growth

21

22 **Plain Language Summary:**

23 Warm-temperature induced REVEILLE 5 (RVE5) impedes hypocotyl growth
24 through competing with CCA1 in joint repression tuning of *ELF4*-induced
25 inhibition of thermo-responsive growth in Arabidopsis.

26

27 **Summary**

- 28 ● Global warming has profound impact on growth and development, and
29 plants constantly adjust their internal circadian clock to cope with external
30 environment. However, how clock-associated genes fine-tune
31 thermoresponsive growth in plants is still less understood.
- 32 ● We found that loss-of-function mutation of *REVEILLE5* (*RVE5*) reduces the
33 expression of circadian gene *EARLY FLOWERING 4* (*ELF4*) in *Arabidopsis*,
34 and confers accelerated hypocotyl growth under warm-temperature
35 conditions.
- 36 ● Both *RVE5* and CIRCADIAN CLOCK ASSOCIATED 1 (*CCA1*) accumulate
37 at warm temperatures and bind to the same EE *cis*-element presented on
38 *ELF4* promoter, but the transcriptional repression activity of *RVE5* is
39 weaker than that of *CCA1*.
- 40 ● The binding of *CCA1* to *ELF4* promoter is enhanced in the *rve5-2* mutant
41 at warm temperatures, and overexpression of *ELF4* in the *rve5-2* mutant
42 background suppresses the *rve5-2* mutant phenotype at warm
43 temperatures.
- 44 ● Therefore, the transcriptional repressor *RVE5* finetunes *ELF4* expression
45 via competing at a *cis*-element with the stronger transcriptional repressor
46 *CCA1* at warm temperatures. Such a competition-attenuation mechanism
47 provides a balancing system for modulating the level of *ELF4* and
48 thermoresponsive hypocotyl growth under warm temperature conditions.

49

50 **Keywords:** *Arabidopsis thaliana*, Hypocotyl growth, Thermomorphogenesis,

51 Warm temperature

52

53

54 **Introduction**

55 Plants have evolved an internal timing keeping-mechanism known as the
56 circadian clock that enables anticipation of external environmental cues to
57 adjust growth and development (Huang & Nusinow, 2016). This clock consists
58 of the input and output pathways, and the central oscillator (Creux & Harmer,
59 2019). Ambient light and temperature cues are two major inputting signals that
60 function at both transcriptional and post-translational levels to set (entrain) this
61 clock (Hsu & Harmer, 2014). The central oscillator at ambient temperature
62 contains multiple repressors and activators that form interconnected feedback
63 loops. Briefly, the morning expressed *CCA1* and *LATE ELONGATED*
64 *HYPOCOTYL (LHY)* repress the expression of afternoon genes *PSEUDO-*
65 *RESPONSE REGULATOR1 (PRR1/TIMING OF CAB EXPRESSION1 (TOC1)*,
66 *PRR5*, *PRR7*, and *PRR9*; in turn, the latter encoded proteins inhibit the
67 expression of former genes *CCA1/LHY* (Alabadi *et al.*, 2001; Kamioka *et al.*,
68 2016). *CCA1/LHY* also inhibit the expression of evening genes of the Evening
69 Complex (EC); and EC represses the expression of PRRs (Herrero *et al.*, 2012;
70 Mizuno *et al.*, 2014). In addition, midday-expressed *REVEILLE 4/6/8*
71 (*RVE4/6/8*) activate the expression of *TOC1*, *PRR5*, and EC genes, but *RVE8*
72 expression is inhibited by *TOC1* and other PRRs (Rawat *et al.*, 2011; Hsu *et al.*,
73 2013; Hsu & Harmer, 2014). Further, *GIGANTEA (GI)* promotes the expression
74 of *CCA1/LHY* whereas *CCA1/LHY* inhibits the expression of *GI* and *TOC1*
75 (Fowler *et al.*, 1999; Mizoguchi *et al.*, 2002). These multiple feedback loops
76 provide rhythmic robustness across dynamic environmental conditions (Shalit-
77 Kaneh *et al.*, 2018). As output pathways, the circadian clock regulates diurnal
78 hypocotyl growth and photoperiod-dependent flowering (Farre, 2012).

79 Global warming has world-wide impacts on plant distribution and crop
80 productivity (Lesk *et al.*, 2016). The plant circadian clock also controls hypocotyl
81 growth under warm-temperature conditions, in a process termed

82 thermomorphogenesis, in which plants sense and adapt to ambient warm
83 temperatures (Park *et al.*, 2021). Several proteins/RNAs have been proposed
84 to be warm temperature sensors in plants. For example, phytochrome B (phyB),
85 originally characterized as a photoreceptor (Lin *et al.*, 2020), is a temperature
86 sensor. Warm temperature accelerates the conversion of phyB from active Pfr
87 to inactive Pr, which reduces the inhibitory effects of phyB on a bHLH
88 transcription factor phytochrome interacting factor 4 (PIF4) (Jung *et al.*, 2016;
89 Legris *et al.*, 2016). PIF4 is the central regulator of plant thermomorphogenesis
90 and subjected to multiple regulation both at transcriptional and post-
91 translational levels (Vu *et al.*, 2019). It recognizes G-box (CACGTG)-containing
92 *cis*-elements and regulates the expression of downstream genes involved in
93 auxin biosynthesis and signaling (Franklin *et al.*, 2011; Sun *et al.*, 2012).

94 EARLY FLOWERING3 (ELF3) is another proposed temperature sensor,
95 which undergoes liquid-liquid phase separation at warm temperatures (Jung *et al.*,
96 2020). It is a core component of the circadian clock and assembles into EC
97 together with ELF4 and LUX ARRHYTHMO (LUX) (Thines & Harmon, 2010;
98 Nusinow *et al.*, 2011; Huang & Nusinow, 2016). ELF4 binding to ELF3 recruits
99 to a nuclear structure {Herrero, 2012 #7;Kolmos, 2011 #58} associated to
100 activity {Anwer, 2014 #63;Ronald, 2022 #64;Ronald, 2021 #62}. Allelic variation
101 within ELF3 has revealed that the presence of these nuclear foci correlates with
102 both circadian function {Anwer, 2014 #63} and thermomorphogenesis
103 {Raschke, 2015 #61}. Indeed, under warm conditions ELF3 disassociates from
104 these active form {Ronald, 2021 #62}, as do phyB signals {Kolmos, 2011
105 #58;Ronald, 2022 #64}.

106 EC binds to the promoter of *PIF4/5* to inhibit gene expression, and such
107 inhibition is reduced under warm temperature conditions (Nomoto *et al.*, 2012;
108 Box *et al.*, 2015; Jung *et al.*, 2020; Silva *et al.*, 2020). Further, the EC plays a
109 major role in directly coordinating the expression of hundreds of key regulators

110 of photosynthesis, the circadian clock, phytohormone signaling, growth and
111 response to the environment (Ezer *et al.*, 2017). In addition, ELF3 also interacts
112 with PIF4 protein and suppresses the transcriptional activity of PIF4 in an EC-
113 independent manner (Nieto *et al.*, 2015). Under warm temperature conditions,
114 ELF3 is subjected to ubiquitination-mediated protein degradation (Ding *et al.*,
115 2018; Zhang *et al.*, 2021a; Zhang *et al.*, 2021c). LUX is a strong DNA-binding
116 MYB transcription factor while the LUX-ELF3 complex is a relatively poor binder
117 of DNA, but its binding activity is much enhanced by adding ELF4 to the
118 complex during *in vitro* assays (Silva *et al.*, 2020). This has been interpreted as
119 that ELF4 acts a modulator of thermomorphogenesis. Indeed, ELF4 protein
120 moves from shoots to regulate rhythms in roots in a temperature-dependent
121 manner (Chen *et al.*, 2020). However, how the ELF4 activity is regulated in
122 plants during thermomorphogenesis is less understood. Relevance here is that
123 increased ELF4 levels generates more ELF3 activity {Herrero, 2012
124 #60;Kolmos, 2009 #47;McWatters, 2007 #65}. We thus hypothesized that a
125 component of thermomorphogenesis would be regulation of ELF4 levels.

126 In this paper, we report the essential role of RVE5 in inhibiting hypocotyl
127 growth at warm temperatures in *Arabidopsis*. We demonstrate that the
128 transcriptional repressor RVE5 maintains *ELF4* expression at warm
129 temperatures via competing with another transcriptional repressor CCA1, in
130 which both RVE5 and CCA1 bind to the same *cis*-element presented on the
131 *ELF4* promoter. As RVE5 has a weaker transcription repression activity relative
132 to that of CCA1, the *rve5* mutant thus has more CCA1 activity leading to
133 increased growth in warmth.

134

135 **Materials and methods**

136 **Plant materials and hypocotyl length measurements**

137 The *rve5-2* T-DNA mutant (GK_225C06) was obtained from the Nottingham
138 *Arabidopsis* Stock Centre (NASC). *pif4-101* was previously described (Ding *et*

139 *al.*, 2018). For the genetic complementation experiment, genomic sequences
140 of *RVE5* including 1.8 kb upstream promoter sequences were amplified and
141 subcloned into pCambia1300, and introduced to the *rve5-2* mutant background
142 via an *Agrobacterium*-mediated floral dip method (Clough & Bent, 1998). For
143 *RVE5* overexpression, the coding region (CDS) of *RVE5* cDNA was amplified
144 and subcloned into pSKM36 and introduced to the wild-type (WT) background
145 to express *RVE5-MYC* driven by the 35S promoter. For *CCA1-FLAG*
146 expression, the promoter (1.6 kb) sequences and CDS sequence of *CCA1* were
147 amplified and subcloned into pCambia1300 in which the *FLAG* sequence was
148 previously inserted, respectively, and the vector was introduced to the WT and
149 *rve5-2* mutant background to produce the *CCA1-FLAG* fusion protein,
150 respectively. For *ELF4* overexpression, the promoter (0.9 kb) sequence of
151 HSP70 (AT3G12580) and CDS sequence of *ELF4* were amplified and
152 subcloned into pCambia1300, respectively, and the vector was introduced to
153 the WT and *rve5-2* mutant background, respectively. All the primers used to
154 generate these constructions are provided in Table S1.

155 Seeds were surface sterilized with 50% ethanol for 1 min and then with 0.01%
156 sodium hypochlorite solutions for 25 min, and subsequently washed with
157 sterilized water for four times. All the seeds were sown directly on half-strength
158 Murashige and Skoog (MS) medium (containing 1.2% sucrose and 0.6% agar,
159 pH adjusted to 5.7), stratified at 4°C for 3 days, and then transferred to a
160 standard plant incubator with the following settings: 22°C, white light
161 100 $\mu\text{mol}/\text{m}^2/\text{s}$, 16/8-hr day/night for 3 days, after which the plates were placed
162 at 22°C or 29°C for 3-4 days, respectively. Plants were photographed and
163 hypocotyl length was measured using ImageJ software (National Institutes of
164 Health).

165 **ChIP-Seq and ChIP-qPCR**

166 ChIP assays were carried out following an integrated method with Chelex resin-
167 based ChIP procedure and protein A agarose beads (Millipore, CA, USA) (Song
168 *et al.*, 2015). Briefly, 14-day-old 35S:*RVE5-MYC/CCA1:CCA1-FLAG*
169 overexpression plants were treated at 22°C or 29°C for the indicated time and
170 sampled for fixation with 1% formaldehyde for 15 min, which was stopped by
171 adding 0.15 M Glycine. After sonication in 0.8% SDS buffer, the mix was
172 immunoprecipitated with *anti-MYC* antibody (Abmart), or *anti-FLAG* antibody
173 (Abmart), or *anti-GST* (Abmart) as the IgG control. ChIP-Seq was performed
174 with an illumina Novaseq™ 6000 (Genergy Bio, Shanghai, China), with details
175 described previously (Gao *et al.*). Briefly, low quality and linker sequence
176 fragments were removed and sequences less than 50 bp were filtered with
177 Skewer. After that, unique mapping of high-quality reads to the reference
178 genome was performed with Bowtie. Peak calling was performed with MACS
179 and the binding peaks were obtained when comparing to that with the input
180 sample ($P < 0.001$). The related genes with common binding peak region in the
181 upstream 2 K in three replicates were considered as the targets of RVE5. The
182 common binding *cis*-elements were identified using MEME. The specific and
183 overlapping targets between RVE5 and CCA1 were shown in Venn diagram,
184 and a hypergeometric probability test of overlapping degree was performed
185 using R. The ChIP-Seq data is deposited in the Gene Expression Omnibus
186 (GEO) under accession number GSE180381. ChIP-qPCR was performed with
187 three biological replicates. All the primers used for ChIP-qPCR are listed in
188 Table S1.

189 **Electrophoretic Mobility Shift Assays (EMSA)**

190 The CDS of *RVE5* and *CCA1* was subcloned into pETMAL-H to produce MBP-
191 RVE5 and MBP-CCA1 recombinant proteins, respectively. The EE-element (5'-
192 AAATATCT-3') derived from the *ELF4* promoter was synthesized and
193 biotinylated with the Biotin 3'-end DNA Labelling Kit (Thermo Fisher Scientific).

194 A mutated EE form (5'-AAATCGAG-3') was used for the competition
195 experiment. EMSA was performed using a LightShift Chemiluminescent EMSA
196 Kit (Thermo Fisher Scientific), according to the manufacturer's protocols. Briefly,
197 each binding reaction (20 mM HEPES, pH 7.2, 80 mM KCl, 0.1 mM EDTA, 10%
198 glycerol, 2.5 mM DTT, 0.07 mg/ mL BSA, 8 ng/mL poly dl-dC) was set at room
199 temperature for 20 min and run on a 5% non-denaturing polyacrylamide gel.
200 After transferring to a nylon membrane (GE), the blot was UV light cross-linked,
201 detected with the Chemiluminescent Nucleic Acid Detection Module (Thermo
202 Fisher Scientific).

203 **Luciferase assays and effector-reporter assays**

204 For bioluminescence assay of the circadian rhythm, the promoter sequence of
205 *CCR2* (1.3 kb) was amplified and inserted into pGreenII 0800, and then the
206 fragment containing the promoter and firefly luciferase (*LUC*) gene sequences
207 was subcloned into pCambia1300, which was introduced to the WT and *rve5*-
208 2 mutant background, respectively. For luciferase measurement, 5-day-old
209 transgenic seedlings (17-19 plants) grown at 22°C (12 hr/12 hr day/night) were
210 kept at 22°C or transferred to 29°C for one day, and then subjected to automatic
211 luciferase measurement using a digital CCD camera for 4 days in continuous
212 light after sprayed with 1 mM luciferin. Period was calculated by fast Fourier
213 transform-nonlinear least squares (FFT-NLLS) provided by BRASS. Student's
214 t-test was performed for statistical analysis. The experiments were performed
215 for three times and similar results were obtained. For effector-reporter assays,
216 sequences of the *ELF4* or *LexA* promoter were synthesized and inserted into
217 pGreen0800-II with the 35S promoter included before the firefly luciferase gene
218 to generate the reporter vector in which the renilla luciferase gene was driven
219 by the 35S promoter. The coding sequence of *LexA-RVE5* or *LexA-CCA1* or
220 *RVE5* or *CCA1* was inserted into the pCAMBIA1300-35S or pSKM36 vector to
221 generate the effector vector. Different combination of constructs was transiently

222 expressed in tobacco (*Nicotiana benthamiana*) leaves via *Agrobacterium*
223 *tumefaciens* strain GV3101. Three days after infiltration, luciferase activities
224 were measured with a dual-luciferase reporter assay kit (Promega). All the
225 primers are listed in Table S1.

226 **RT-qPCR and western blotting analysis**

227 For RT-qPCR, total RNAs were extracted with three biological replicates using
228 an RNA Prep Pure Plant kit (Tiangen) and reverse transcribed using
229 5×PrimeScript RT Master Mix (Takara) and oligo (dT) primers. RT-qPCR was
230 performed using SuperReal PreMix Color (Tiangen) in a CFX96 real-time
231 system (Bio-Rad). $\Delta\Delta C_t$ (threshold cycle) method was applied to calculate the
232 gene expression. All the primers used are listed in Table S1. Western blotting
233 was performed as described (Zhang *et al.*, 2021c). Total proteins were
234 extracted with the extraction buffer (125 mM Tris-HCl, pH 8.0, 375 mM NaCl,
235 2.5 mM EDTA, 1% SDS and 1% β -mercaptoethanol). Afterward, proteins were
236 separated in 4-20% SDS-PAGE gels and analyzed using *anti*-FLAG(Abmart),
237 *anti*-MYC(Abmart), *anti*-tubulin (Abmart), respectively. Each immunoblot was
238 quantified using ImageJ software.

239

240 **Results**

241 **RVE5 inhibits thermoresponsive hypocotyl elongation in *Arabidopsis***

242 The RVE family proteins (RVE1 to RVE8) are morning-phased MYB-like
243 transcription factors at ambient temperature that are homologous to the central
244 clock genes CCA1 and LHY (Kuno *et al.*, 2003; Rawat *et al.*, 2009). In our
245 previous study on transcriptomic analysis of heat stress responses in
246 *Arabidopsis*, we found that *RVE5* was a lone RVE increased in expression by
247 warming temperature (Zhang *et al.*, 2017). To explore if RVE5 is involved in
248 warm temperature-mediated growth, we obtained a null mutant *rve5-2* with the
249 T-DNA inserted in the first exon of *RVE5*, and the MYB DNA-binding domain of

250 RVE5 is predicted to be disrupted in the *rev5-2* mutant (Fig. S1a-b), and
251 performed phenotypic analyses. We first checked the hypocotyl growth of WT
252 and *rve5-2* mutant plants under both ambient (22°C) and warm (29°C)
253 temperature conditions. The *rve5-2* mutant plants had a similar hypocotyl length
254 as the WT plants at 22°C. In contrast, when compared with that of the WT, the
255 hypocotyl length of *rve5-2* mutant was significantly taller at 29°C (Fig. 1a-b).
256 The thermoresponsive hypocotyl phenotype of *rve5-2* mutant was rescued by
257 introducing the genomic sequence of *RVE5* in three independent transgenic
258 lines (Fig. 1a-b). This transgenic complementation confirms the important role
259 of *RVE5* in plant thermomorphogenesis. We also generated 35S:*RVE5-MYC*
260 overexpression plants (Fig. S2a-c). Consistent with *RVE5* functioning to
261 suppress growth under warmth, the hypocotyl length of the overexpression
262 plants (*RVE5ox*) was slightly shorter than that of the WT plants under warm
263 temperature conditions (Fig. S2a-b). Although the expression of *RVE5* was
264 found to be high in these transgenic plants (Fig. S2c), *RVE5* protein
265 accumulation may not have been sufficient for a stronger hypocotyl phenotype.
266 We further checked the hypocotyl phenotype of *rve5-2* mutant and genetically
267 complemented transgenic plants at both 22°C and 29°C in darkness, and the
268 results showed that there were no obvious differences among these plant
269 materials in terms of hypocotyl growth (Fig. S3), suggesting that the function of
270 *RVE5* in thermomorphogenesis is dependent on light. Thus, *RVE5* is a negative
271 regulator of thermomorphogenesis and essential for controlling hypocotyl
272 growth at warm temperatures.

273 The bHLH transcription factor *PIF4* is a central regulator of plant
274 thermomorphogenesis (Koini *et al.*, 2009; Quint *et al.*, 2016). To analyze the
275 genetic relationship between *RVE5* and *PIF4*, we generated the double mutant
276 *rve5-2 pif4-101* and carried out epistatic analyses. Opposite to the *rve5-2* single
277 mutant, but similar to the *pif4-101* single mutant, the hypocotyl of *rve5-2 pif4-*

278 101 plants did not substantially elongate at 29°C (Fig. 1c-d). Thus, *PIF4* was
279 found to be epistatic to *RVE5* during thermomorphogenesis. Taken together,
280 these results support that *RVE5* functions upstream of *PIF4* in
281 thermomorphogenesis.

282 **RVE5 shares genome-wide direct targets with CCA1**

283 To next explore the mechanism of *RVE5* in controlling thermoresponsive
284 growth, we performed biochemical analysis and Chromatin
285 Immunoprecipitation-Sequencing (ChIP-Seq). Firstly, we checked the protein
286 stability of *RVE5* under warm temperature conditions with 35S:*RVE5-MYC*
287 overexpression plants (*RVE5ox-4*). Western blotting showed that the protein
288 level of *RVE5-MYC* was increased at 29°C comparing to that at 22°C (Fig. 2a).
289 Using these *RVE5-MYC* overexpression plants grown at 29°C, we performed
290 ChIP-Seq to examine chromatin occupancy of *RVE5*. The normalized IP signals
291 were peaked in the promoter regions (Fig. 2b), representing a typical
292 transcription factor binding characteristic. In total, 385 loci were identified that
293 are enriched in all of the three replicates (Table S2). Hereafter we refer them
294 as *RVE5*-targets. The *cis*-elements Evening Element (EE) responsible for
295 rhythmic gene expression (Nagel *et al.*, 2015) and G-box were highly enriched
296 in these binding peaks (Fig. 2c-d). Because *RVE5* is a protein with sequence
297 similarity to *CCA1*, we compared *RVE5* targets to previously identified *CCA1*
298 targets (Kamioka *et al.*, 2016). We found that *RVE5* and *CCA1* significantly
299 shared overlapping targets ($P=3.6e-156$) at 175 gene loci (Fig. 2e and Table
300 S2). Together, these results support that *RVE5* shares some common direct
301 targets with *CCA1*.

302 **RVE5 binds to the promoter of clock-associated genes and regulates their** 303 **expression under warm temperature conditions**

304 The ChIP-Seq data revealed that *RVE5* was enriched in the promoter regions
305 of many circadian clock genes, including *ELF4*, *LUX*, *TOC1*, *GI*, *PRR5*, *PRR7*,

306 and *CCR2* (Fig. 2f). However, RVE5 was hardly detected at the promoter of
307 *ELF3*, *CCA1*, *LHY1*, *PRR9* and *PIF4* (Fig. 2f). To check the effect of
308 temperature conditions on RVE5-binding to these direct targets, we selected
309 *ELF4*, *PRR5* and *PRR7*, and performed ChIP-qPCR to confirm and further
310 compare the RVE5-binding at both 22°C and 29°C. The results confirmed the
311 ChIP-Seq data and showed that warm temperature enhanced the binding of
312 RVE5 to the promoter of *ELF4*, *PRR5*, and *PRR7* (Fig. 2g-i).

313 To examine whether RVE5 regulates the timed expression of its target
314 clock genes, we carried out RT-qPCR to monitor gene expression at multiple
315 time points within two days under two different temperature conditions in the
316 WT and *rve5-2* mutant plants. The results showed that the expression of *ELF4*,
317 *CCA1*, *LHY1*, *PRR9*, *PRR7*, *PRR5*, *TOC1*, *GI*, and *CRR2* was affected in the
318 *rve5-2* mutant at 29°C at least at one timepoint when compared to that of the
319 WT plants, while the expression of *ELF3* and *LUX* was not appreciably affected
320 in the *rve5-2* mutant (Fig. 3). For example, there was no obvious difference in
321 the expression level of *ELF4* at 22°C between WT and *rve5-2* mutant, however,
322 the expression of *ELF4* was much lower in *rve5-2* mutant than that in WT plants
323 at 29°C at ZT 12 hr and ZT 36 hr (Fig. 3). These results suggest that RVE5
324 controls the expression of *ELF4* and other clock genes under warm temperature
325 conditions.

326 The expression of *PIF4* was increased in *rve5-2* mutant plants when
327 compared to that in WT plants at 29°C at ZT 12 hr, ZT 16 hr, ZT 36 hr, and ZT
328 40 hr (Fig. 3), which is consistent with the lower level of *ELF4* expression and
329 longer hypocotyl phenotype of *rve5-2* mutant plants at 29°C. We also checked
330 the expression of *PIF4* downstream genes (Wang *et al.*, 2018), and found that
331 the transcript levels of *YUCCA 8* (*YUC8*, At4g28720), Indole-3-Acetic Acid 19
332 (*IAA19*, At3g15540), and *XYLOGLUCAN ENDOTRANSGLYCOSYLASE 7*
333 (*XTR7*, At4g14130) were higher in *rve5-2* mutant plants at 29°C compared to

334 that in WT plants (Fig. S4). The expression of these PIF4 downstream genes
335 were strongly affected in the *rve5-2* mutant, suggesting that PIF4 may also
336 subjected to RVE5-dependent post-translational modifications at warm
337 temperature. PRR5 is known to interact with PIF4 and repress its
338 transactivation activity (Zhu *et al.*, 2016). Indeed, the expression of *PRR5* was
339 also affected in the *rve5-2* mutant comparing to that in the WT plants (Fig. 3).
340 Therefore, we do not exclude the possibility that RVE5 functions through PIF4
341 post-translationally. It is known that EC inhibits the expression of *PIF4* (Nomoto
342 *et al.*, 2012; Box *et al.*, 2015; Silva *et al.*, 2020), therefore, we focused on the
343 regulation of *ELF4* expression by RVE5 at warm temperature in the later study.
344 In addition, the phase of the expression of many of the tested clock genes was
345 delayed (Fig. 3). Therefore, we examined activity of the circadian-regulated
346 *CCR2::LUC* reporter in WT and *rve5-2* mutant background. Comparing to that
347 in WT plants, delayed phase was observed in *rve5-2* mutant plants at 29°C (Fig.
348 S5a-f), and the period of circadian clock was a little bit lengthened in *rve5-2*
349 mutant plants, especially at 29°C (Fig. S5a-f). Taken together, these results
350 demonstrate that RVE5 regulates the expression of clock genes such as *ELF4*
351 under warm temperature conditions.

352 **RVE5 has a weaker transcriptional repression activity when comparing** 353 **with CCA1**

354 As the EE *cis*-element (AAATATCT) was shown to be enriched in the binding
355 peaks of RVE5 (Fig. 2c), to examine whether RVE5 regulates the expression
356 of *ELF4* through the EE *cis*-element, electrophoretic mobility shift assays
357 (EMSAs) were performed with the recombinant purified MBP-RVE5. Similar to
358 MBP-CCA1, when MBP-RVE5 was incubated with the biotin-labelled EE
359 identified from the promoter of *ELF4*, a band shift was observed (Fig. 4a-b),
360 reflecting the formation of protein-DNA complexes. Adding non-labeled cold
361 probes could compete the binding while adding the mutated form of cold probes

362 could not (Fig. 4a-b). This revealed the binding-specificity of RVE5 to *ELF4*-
363 promoter DNA.

364 Our subcellular localization study confirmed that RVE5-YFP localizes in
365 the nucleus (Fig. S6). To examine whether RVE5 has transcriptional activation
366 or repressor activity, we firstly checked this in yeast cells. In contrast to the
367 positive control, we did not observe any transcriptional activation activity
368 associated with RVE5 (Fig. 4c). Therefore, we checked the possible
369 transcriptional repressor activity of RVE5 in a LexA-based effector-reporter
370 system (Lin & Little, 1989), in which a LexA fusion protein recognizes the *cis*-
371 element presented on the LexA promoter/operator (pLexA) through the DNA-
372 binding domain of LexA (Fig. 4d). Similar to CCA1, RVE5 had transcriptional
373 repression activity because the LexA-RVE5 fusion protein repressed the
374 reporter activity (Fig. 4e). Notably, RVE5 had a weaker repression activity than
375 CCA1 (Fig. 4e). Using the promoter sequences of *ELF4* containing the EE *cis*-
376 element (AAATATCT) in the effector-reporter assays, we confirmed that RVE5
377 indeed had a weaker transcriptional repression activity than CCA1 in terms of
378 regulating the activity of *ELF4* promoter in plants (Fig. 4f-g). Therefore, RVE5
379 is a transcriptional repressor and has a weaker repression activity than CCA1.

380 **RVE5 competes with CCA1 and reduces the CCA1-binding to *ELF4*** 381 **promoter under warm temperature conditions**

382 To examine how RVE5 affects the function of CCA1 in thermomorphogenesis,
383 we expressed FLAG-tagged form of CCA1 with its native *CCA1* promoter in
384 both WT and *rve5-2* mutant backgrounds and two independent transgenic lines
385 with comparable CCA1-FLAG protein level in each genetic background were
386 selected for later studies (Fig. 5a-f). Although *CCA1* expression and CCA1
387 protein accumulation in WT plants were low at ZT 12 hr at ambient temperature
388 (Fig. 3 & 5a), CCA1 protein was accumulated at ZT 12 hr at warm temperatures
389 in both genetic backgrounds (Fig. 5a-b). We performed ChIP-qPCR using

390 *CCA1:CCA1-FLAG* expressing plants grown only at 29°C at ZT 12 hr because
391 the protein level of *CCA1-FLAG* was low at 22°C at ZT 12 hr. The results
392 showed that *CCA1-FLAG* was more enriched in the promoter regions of *ELF4*
393 containing the EE *cis*-element in the *rve5-2* mutant background than that in the
394 WT background (Fig. 5g-h), which is consistent with the results that the
395 expression level of *ELF4* was lower while that of *PIF4* was higher in the
396 *CCA1:CCA1-FLAG* expressing plants in *rve5-2* mutant background than that in
397 the WT background (Fig. 6a-d). We also performed ChIP-PCR at ZT 4 hr when
398 *CCA1* protein abundance was higher than that at ZT 12 hr (Fig. 5a-b). The
399 results showed that the difference of *CCA1*-binding to *ELF4* promoter in
400 between WT and *rve5-2* mutant at ZT 4 hr was reduced than that at ZT 12 hr
401 (Fig. S7). These results demonstrate that *RVE5* competes with *CCA1* in binding
402 to *ELF4* promoter in the evening to regulate the expression of *ELF4* and its
403 downstream target *PIF4*.

404 *LHY* is partially redundant to *CCA1* in terms of controlling circadian clock
405 and hypocotyl growth in *Arabidopsis* (Mizoguchi *et al.*, 2002). To explore the
406 genetic relationship between *RVE5* and *CCA/LHY*, we crossed *rve5-2* to *cca1-1*
407 *lhy-20* (Marshall *et al.*, 2016) to generate the *rve5-2 cca1-1* double mutant
408 and the *rve5-2 cca1-1 lhy-20* triple mutant, and examined their hypocotyl
409 elongation phenotypes. Under ambient temperature conditions, hypocotyl
410 length of all the examined plant materials was similar (Fig. 6f-h). Under warm
411 temperature conditions, the hypocotyl length of *cca1-1* mutant was similar to
412 that of WT plants, while the hypocotyl length of *rve5-2* mutant was taller than
413 that of WT plants at warm temperatures, however, mutation of *CCA1*
414 suppressed the hypocotyl phenotype of *rve5-2* mutant (Fig. 6e & g). The
415 hypocotyl length of *cca1-1 lhy-20* double mutant plants was shorter than that of
416 WT plants, while the hypocotyl phenotype of *rve5-2* mutant was also
417 suppressed in the *rve5-2 cca1-1 lhy-20* triple mutant plants under warm

418 temperature conditions (Fig. 6f & h), suggesting that the function of *RVE5* in
419 thermomorphogenesis is partially dependent on *CCA1/LHY*. These results are
420 consistent with that *RVE5* is competitive to *CCA1* and perhaps also to *LHY*
421 during hypocotyl elongation under warm temperature conditions.

422 The expression level of *ELF4* transcript was decreased in *rve5-2* mutant
423 plants under warm temperature conditions (Fig. 3). To investigate whether such
424 decrease in *ELF4* gene expression contributed to the observed *rve5-2* mutant
425 phenotype. We overexpressed *ELF4* in the WT and *rve5-2* mutant backgrounds,
426 respectively, and selected two independent lines with comparable transgenic
427 expression level. Overexpression of *ELF4* in the WT background reduced
428 hypocotyl growth at 29°C, in contrast, overexpression of *ELF4* in the *rve5-2*
429 mutant background rescued the long hypocotyl phenotype of *rve5-2* mutant
430 plants at 29°C (Fig. 7a-c). EC inhibits the expression of *PIF4* (Nomoto *et al.*,
431 2012), therefore, we also checked the expression level of *PIF4* in these plant
432 materials. Agreed with the observed hypocotyl phenotypes, the expression of
433 *PIF4* was increased in *rve5-2* mutant while decreased in *ELF4* overexpression
434 plants (WT background) at 29°C, suggesting that high level of *ELF4* inhibits
435 *PIF4* expression and suppresses hypocotyl elongation. In contrast, *ELF4*
436 overexpression reduced the expression level of *PIF4* in *rve5-2* mutant
437 background (Fig. 7d). We also crossed *rve5-2* mutant to *elf4-209* null mutant
438 (Kolmos *et al.*, 2009) to generate the *rve5-2 elf4-209* double mutant. The
439 hypocotyl length of *rve5-2 elf4-209* double mutant was similar to that of *elf4-*
440 *209* single mutant at both 22°C and 29°C (Fig. 7e-f), suggesting that *ELF4* is
441 epistatic to *RVE5*. The expression level of *PIF4* in *rve5-2 elf4-209* double
442 mutant was also similar to that in *elf4-209* mutant plants (Fig. 7g). Taken
443 together, these results demonstrated that *RVE5* functions upstream of *ELF4* to
444 modulate the expression level of *ELF4* and its downstream gene *PIF4* for
445 regulating hypocotyl growth at warm temperatures.

446

447 **Discussion**

448 Plants have evolved many strategies to better adapt to their given environment.
449 For example, plants have a faster hypocotyl elongation, hyponastic leaf growth
450 and accelerated flowering at warm temperatures (Vu *et al.*, 2019). During
451 thermomorphogenesis, the bHLH transcription factor PIF4 is a central hub for
452 integrating the warm temperature signals to regulate downstream gene
453 expression involved in plant morphogenesis (Casal & Balasubramanian, 2019).
454 Recently studies have revealed the important role of ELF3, one of the EC
455 components, in inhibiting PIF4 protein activity both transcriptionally and post-
456 translationally (Nomoto *et al.*, 2012; Nieto *et al.*, 2015). In the current study, we
457 demonstrated that RVE5 regulates thermoresponsive hypocotyl growth through
458 regulating the expression level of *ELF4*, encoding another EC component ELF4
459 in *Arabidopsis*, although we do not exclude the possibility that RVE5 also
460 regulated the expression of other clock genes under warm temperature
461 conditions.

462 In our working model (Fig. 8), RVE5 and CCA1 bind to the same *cis*-element
463 presented on the promoter of *ELF4* under warm temperature conditions, but
464 RVE5 has a weaker transcriptional repression activity than CCA1 (Fig. 4). This
465 competition-attenuation model (Fig. 8) considers that the circadian-controlled
466 CCA1 and LHY proteins directly suppress *ELF4* expression periodically at dawn
467 at ambient temperature (Li *et al.*, 2011). CCA1 level is increased in response
468 to warm temperatures in WT plants (Fig. 5a-f), however, RVE5 is also increased
469 under warm temperature conditions (Fig. 2a) to reduce the inhibitory effect of
470 CCA1/LHY on *ELF4* expression, therefore, the expression level of *ELF4* is
471 maintained to a relatively high homeostatic level (Fig. 3). The encoding ELF4
472 protein incorporates into the EC {Herrero, 2012 #60}, which inhibits the
473 expression of *PIF4* (Nomoto *et al.*, 2012). In the *rve5-2* mutant plants, higher

474 occupancy of CCA1 at the *ELF4* promoter given of the absence of RVE5 (Fig.
475 5g-h) Thus counter intuitively for the removal of the RVE5 repressor of *ELF4*,
476 this results in a reduced expression of *ELF4* (Fig. 6a), which leads to elevated
477 *PIF4* expression (Fig. 6b) and promotes taller hypocotyls under warm
478 temperature conditions (Fig. 1a-b).

479 The EC activity is finely tuned at warm temperature (Zhang *et al.*, 2021b).
480 Recently, we demonstrated that ELF3 protein level is subjected to proteolysis
481 mediated by XBAT31/35 under warm temperature conditions (Zhang *et al.*,
482 2021a; Zhang *et al.*, 2021c). Functional ELF3 structures also disapeate under
483 warming conditions {Ronald, 2021 #62}, and ELF4 is known to convey thermal
484 information {Chen, 2020 #33}. Our results here demonstrated that maintaining
485 *ELF4* expression by RVE5 during the daytime (evening) is also important for
486 controlling hypocotyl growth at warm temperatures in *Arabidopsis*. Since RVE5
487 directly binds to promoters of other clock genes and regulates the expression
488 of many clock genes, we do not exclude the possibility that RVE5 also functions
489 in thermomorphogenesis during the night-time period at warm temperature
490 through other unknown mechanisms.

491 While CCA1 and LHY are deemed core members of the circadian clock,
492 RVE1, RVE3 and RVE5 play a modest role in controlling clock under prevailing
493 ambient temperature conditions (Gray *et al.*, 2017). In the current study, we
494 found that RVE5 functions in regulating the circadian gene expression under
495 warm-temperature conditions (Fig. 3), further the understanding of RVE5 in
496 controlling the circadian clock at warm temperatures. Our ChIP-Seq experiment
497 showed that many clock-related genes are also direct targets of RVE5 (Fig. 2),
498 suggesting that RVE5 is involved in circadian clock function itself. Indeed, our
499 circadian reporter *CCR2::LUC* experiments demonstrate that mutation of *RVE5*
500 leads to long-period and phase delay under warm temperature conditions (Fig.
501 S3).

502 CCA1 is critical in regulating thermoresponsive hypocotyl growth, as
503 expression of *ELF4* is impaired only in *rve5-2* mutant at 29°C (Fig. 3). The
504 hypocotyl length of *RVE5* overexpression plants was not dramatically affected at
505 29°C (Fig. S2), further suggests that CCA1 has dominant roles in this process.
506 The protein level of CCA1 was increased (Fig, 5a) while the expression of
507 *CCA1* decreased (Fig. 3) under warm temperature conditions. It has been
508 hypothesized that this is because of auto-regulation of CCA1 (Wang & Tobin,
509 1998). CCA1 occupancy of the *ELF4* promoter was found to be increased in
510 *rve5-2* mutant at ZT 12 hr at 29°C (Fig. 5g-h), indicating that temperature-
511 mediated changes in CCA1 stability is central to this control.

512 Protein levels of CCA1 at ZT 12 hr are decreased comparing to that at ZT
513 4 hr (Fig. 5a), while the protein level of RVE5 is constantly increased at 29°C
514 (Fig. 2a). This is consistent with a specificity role of RVE5 at warm temperatures.
515 Indeed RVE5 is the RVE most dramatically regulated by warming {Zhang, 2017
516 #39}. How the protein stability of RVE5 is controlled at warm temperature is
517 currently not known. Sumoylation is a post-translational regulatory process that
518 conjugates small ubiquitin-like modifier (SUMO) proteins to target proteins to
519 enhance protein stability (Miura *et al.*, 2007). Sumoylation of CCA1 was
520 previously reported (Hansen *et al.*, 2017) and RVE5 is predicted to have
521 sumoylation sites. Therefore, it is possible that RVE5 is subjected to
522 sumoylation at warm temperature, which awaits future investigation.

523 Because the *rve5-2* mutant has the long hypocotyl phenotype only at a
524 warm temperature (Fig. 1a-b), we consider that those mis-expressed genes
525 specifically at warm temperatures attributes to the observed hypocotyl
526 phenotype. We do not exclude the possibility that RVE5 has additional
527 biological functions outside of thermomorphogenesis, because there are mis-
528 expressed clock genes in *rve5-2* mutant plants at an ambient temperature. We
529 found a slight increase of *PIF4* expression at 22°C but did not observe the long

530 hypocotyl phenotype in *rve5-2* mutant at 22°C, which can be explained by the
531 multiple regulations of PIF4 at post-translational levels (Zhang *et al.*, 2021b).

532 The underlying molecular mechanism of RVE5's function on gene
533 expression is quite interesting. Both RVE5 and CCA1 have transcriptional
534 repressor activity (Fig. 4), however, CCA1 inhibits while RVE5 maintains *ELF4*
535 expression under warm temperature conditions. It was reported that LNK1 and
536 LNK2 act as coactivators with RVE8 to promote gene expression (Rugnone *et al.*,
537 *et al.*, 2013; Xie *et al.*, 2014). Here in the current study we demonstrate that RVE5
538 maintains gene expression through a novel mechanism. The relative weaker
539 repression activity of RVE5 counteracts with the strong repression activity of
540 CCA1 on the same promoter. This lifts the repression strength of downstream
541 gene expression. LHY is partially redundant to CCA1 and shares direct targets
542 with CCA1 (Mizoguchi *et al.*, 2002; Adams *et al.*, 2018). Among the 722 direct
543 targets of LHY, RVE5 shares 100 target genes including *ELF4* with LHY based
544 on our CHIP-Seq data. Therefore, it is possible that RVE5 also competes with
545 LHY during thermomorphogenesis.

546 In conclusion, our results reveal the important role of RVE5 in
547 thermomorphogenesis, and provide a unique model to explain how the
548 transcriptional repressor RVE5 maintain gene expression during
549 thermomorphogenesis in plants; it is a more modest repressor than a direct
550 competitor. This provides a critical insight into how the circadian clock regulates
551 plant growth to cope with warming temperature changes.

552

553

554 **Supplemental information**

555 **Fig. S1. Validation of *RVE5* T-DNA mutant plants.**

556 (a) Schematic map of the T-DNA insertion positions in the *RVE5* gene. Coding
557 regions, untranslated regions and introns are indicated by the black boxes,

558 white boxes and black lines, respectively. **(b)** Detection of *RVE5* gene
559 expression in wild-type (WT) and *rve5-2* mutant plants by RT-qPCR using
560 primers flanking the T-DNA insertion. The *UBQ5* gene was used as a loading
561 control.

562 **Fig. S2. Phenotypic analysis of *RVE5* overexpression plants.**

563 **(a-b)** Thermoresponsive hypocotyl growth of wild-type (WT) plants and *RVE5*-
564 *MYC* overexpression plants (*RVE5ox-3/RVE5ox-8/RVE5ox-10*). All the
565 materials grown at 22°C were kept at 22°C or transferred to 29°C for 3 days,
566 after which plants were imaged (a) and their hypocotyl lengths were
567 subsequently measured (b). Error bars depict SD (n=22). Letters above the
568 bars indicate significant differences as determined by HSD test ($P < 0.05$). Bar
569 = 5 mm. **(c)** Validation of transgenic lines. WT and *RVE5-MYC* overexpression
570 plants were sampled at ZT12 hr for RT-qPCR analysis of *RVE5* expression.
571 Relative gene expression is the expression level of *RVE5* (total) normalized to
572 that in the sample of WT at 22°C, both of which were normalized to that of *PP2A*.
573 The bars depict the *SE* (n=3).

574 **Fig. S3. Thermoresponsive hypocotyl growth in the dark.** Wild-type (WT)
575 plants, *RVE5* mutant (*rve5-2*), and genetic complemented plants
576 (COM25/COM34/COM29) were grown at 22°C or 29°C in darkness for 3 days
577 and photographed (a), and the hypocotyl length of each plant was subsequently
578 measured (b). Error bars depict SD (n=24). Letters above the bars indicate
579 significant differences as determined by HSD test ($P < 0.05$). Bar = 5 mm.

580 **Fig. S4. Gene expression analysis of PIF4 downstream genes.** Five-day-
581 old Wild-type (WT) and *RVE5* mutant (*rve5-2*) plants grown at 22°C were
582 maintained at 22°C or transferred to 29°C and sampled at three different time
583 points (ZT) for quantitative gene expression analysis. The expression level of
584 each gene was normalized to that of the WT at ZT12 hr at 22°C, which was
585 normalized to that of *PP2A*. Data are means \pm SE (n = 3).

586 **Fig. S5. Effect of *RVE5* mutation on circadian phase and period.**

587 (a-f) Circadian rhythm measurements in WT and *rve5-2* mutant plants. The
588 circadian reporter *CCR2::LUC* was introduced into the WT background (WT)
589 and *rve5-2* background (*rve5-2*), respectively. Two independent transgenic
590 lines (a-c and b-f) in each background were selected. Five-day-old transgenic
591 plants grown at 22°C were kept at 22°C or transferred to 29°C for one day, and
592 then subjected to automatic luciferase measurement (a-b, d-e). Period of clock
593 was calculated (c & f). The bars depict the SD (n=17-19). Asterisks indicate
594 significance levels in Student's t-tests (**P < 0.01, ***P < 0.001).

595 **Fig. S6. Subcellular localization of *RVE5*-YFP.**

596 The YFP-tagged *RVE5* or the empty vector alone (YFP) were transiently
597 expressed in tobacco leaves and observed under YFP channel or bright field.
598 Bar = 50 μm.

599 **Fig. S7. *CCA1*-binding to *ELF4* promoter under warm temperature**
600 **conditions.**

601 (a) Western blotting analysis. *CCA1-FLAG* was expressed with the *CCA1*
602 native promoter in the wild type (WT) or *rve5-2* mutant background. Transgenic
603 plants in the WT background (*CCA1-21*) and *rve5-2* mutant background (*CCA1-*
604 *17*) grown at 29°C were harvested at ZT 4 hr for western-blotting analysis.
605 Tubulin served as a protein-loading control. Signal intensity of each band was
606 quantified and normalized to that of the first sample. Three biological replicates
607 (REP) are shown in the figure. (b) ChIP-qPCR. Plants grown at 29°C were
608 harvested at ZT 4 hr for ChIP-qPCR using *anti-FLAG* antibody. IgG was used
609 as a negative control. Relative enrichment of each sample was normalized to
610 that of IgG sample at 29°C, both of which were normalized to that of the *TA3*
611 control. Error bar represents SE (n = 3).

612

613 **Table S1. Primers used in this study.**

614 **Table S2. Direct targets of RVE5 identified by ChIP-Seq.**

615

616 **Acknowledgements**

617 This project was financially supported by grants from Zhejiang Provincial Talent
618 Program (2019R52005), the Fundamental Research Funds for Zhejiang
619 Provincial Universities (2021XZZX023), National Natural Science Foundation
620 of China (31625004), 111 Project (B14027), and the BBSRC (BB/N018540/1).

621

622 **Author contributions**

623 J.X.L. and W.L. designed the experiments; W. L., Y.Y.T., J.Y.L. L.Y. and L.L.Z.,
624 performed the experiments; J.X.L. W.L. X.D.X. and Z.Y.W. analysed the data;
625 J.X.L., and S.J.D wrote the paper.

626

627 **Declaration of interests**

628 The authors declare no competing interests.

629

630 **References**

- 631 **Adams S, Grundy J, Veflingstad SR, Dyer NP, Hannah MA, Ott S, Carre IA. 2018.**
632 Circadian control of abscisic acid biosynthesis and signalling pathways revealed
633 by genome-wide analysis of LHY binding targets. *New Phytologist* **220**(3): 893-
634 907.
- 635 **Alabadi D, Oyama T, Yanovsky MJ, Harmon FG, Mas P, Kay SA. 2001.** Reciprocal
636 regulation between TOC1 and LHY/CCA1 within the Arabidopsis circadian clock.
637 *Science* **293**(5531): 880-883.
- 638 **Box MS, Huang BE, Domijan M, Jaeger KE, Khattak AK, Yoo SJ, Sedivy EL, Jones DM,**
639 **Hearn TJ, Webb AAR, et al. 2015.** ELF3 controls thermoresponsive growth in
640 Arabidopsis. *Current Biology* **25**(2): 194-199.
- 641 **Casal JJ, Balasubramanian S 2019.** Thermomorphogenesis. Annual Review of Plant
642 Biology, 321-346.
- 643 **Chen WW, Takahashi N, Hirata Y, Ronald J, Porco S, Davis SJ, Nusinow DA, Kay SA,**
644 **Mas P. 2020.** A mobile ELF4 delivers circadian temperature information from
645 shoots to roots. *Nature Plants* **6**(4): 416-426.
- 646 **Clough SJ, Bent AF. 1998.** Floral dip: a simplified method for Agrobacterium-mediated
647 transformation of *Arabidopsis thaliana*. *Plant Journal* **16**(6): 735-743.

648 **Creux N, Harmer S. 2019.** Circadian rhythms in plants. *Cold Spring Harbor Perspectives*
649 *in Biology* **11**(9), a034611.

650 **Ding L, Wang S, Song ZT, Jiang Y, Han JJ, Lu SJ, Li L, Liu JX. 2018.** Two B-box domain
651 proteins, BBX18 and BBX23, interact with ELF3 and regulate
652 thermomorphogenesis in Arabidopsis. *Cell Reports* **25**(7): 1718-1728.

653 **Ezer D, Jung JH, Lan H, Biswas S, Gregoire L, Box MS, Charoensawan V, Cortijo S, Lai**
654 **X, Stockle D, et al. 2017.** The evening complex coordinates environmental and
655 endogenous signals in Arabidopsis. *Nature Plants* **3**:17087.

656 **Farre EM. 2012.** The regulation of plant growth by the circadian clock. *Plant Biology*
657 **14**(3): 401-410.

658 **Fowler S, Lee K, Onouchi H, Samach A, Richardson K, Coupland G, Putterill J. 1999.**
659 GIGANTEA: a circadian clock-controlled gene that regulates photoperiodic
660 flowering in Arabidopsis and encodes a protein with several possible
661 membrane-spanning domains. *EMBO Journal* **18**(17): 4679-4688.

662 **Franklin KA, Lee SH, Patel D, Kumar SV, Spartz AK, Gu C, Ye S, Yu P, Breen G, Cohen**
663 **JD, et al. 2011.** PHYTOCHROME-INTERACTING FACTOR 4 (PIF4) regulates auxin
664 biosynthesis at high temperature. *Proceedings of the National Academy of*
665 *Sciences of the United States of America* **108**(50): 20231-20235.

666 **Gao J, Wang MJ, Wang JJ, Lu HP, Liu JX.** bZIP17 regulates heat stress tolerance at
667 reproductive stage in Arabidopsis. *aBIOTECH* **3**(1): 1-11.

668 **Gray JA, Shalit-Kaneh A, Chu DN, Hsu PY, Harmer SL. 2017.** The REVELLE clock genes
669 inhibit growth of juvenile and adult plants by control of cell size. *Plant*
670 *Physiology* **173**(4): 2308-2322.

671 **Hansen LL, Imrie L, Le Bihan T, van den Burg HA, van Ooijen G. 2017.** Sumoylation of
672 the plant clock transcription factor CCA1 suppresses DNA binding. *Journal of*
673 *Biological Rhythms* **32**(6): 570-582.

674 **Herrero E, Kolmos E, Bujdoso N, Yuan Y, Wang M, Berns MC, Uhlworm H, Coupland**
675 **G, Saini R, Jaskolski M, et al. 2012.** EARLY FLOWERING4 recruitment of EARLY
676 FLOWERING3 in the nucleus sustains the Arabidopsis circadian clock. *Plant Cell*
677 **24**(2): 428-443.

678 **Hsu PY, Devisetty UK, Harmer SL. 2013.** Accurate timekeeping is controlled by a
679 cycling activator in Arabidopsis. *eLife* **2**, e00473.

680 **Hsu PY, Harmer SL. 2014.** Wheels within wheels: the plant circadian system. *Trends in*
681 *Plant Science* **19**(4): 240-249.

682 **Huang H, Nusinow DA. 2016.** Into the Evening: complex interactions in the
683 Arabidopsis circadian clock. *Trends in Genetics* **32**(10): 674-686.

684 **Jung JH, Barbosa AD, Hutin S, Kumita JR, Gao M, Derwort D, Silva CS, Lai X, Pierre E,**
685 **Geng F, et al. 2020.** A prion-like domain in ELF3 functions as a thermosensor
686 in Arabidopsis. *Nature* **585**, 256-260.

687 **Jung JH, Domijan M, Klose C, Biswas S, Ezer D, Gao M, Khattak AK, Box MS,**
688 **Charoensawan V, Cortijo S, et al. 2016.** Phytochromes function as
689 thermosensors in Arabidopsis. *Science* **354**(6314): 886-889.

690 **Kamioka M, Takao S, Suzuki T, Taki K, Higashiyama T, Kinoshita T, Nakamichi N. 2016.**
691 Direct repression of evening genes by CIRCADIAN CLOCK-ASSOCIATED1 in the
692 Arabidopsis circadian clock. *Plant Cell* **28**(3): 696-711.

693 **Koini MA, Alvey L, Allen T, Tilley CA, Harberd NP, Whitelam GC, Franklin KA. 2009.**
694 High temperature-mediated adaptations in plant architecture require the bHLH
695 transcription factor PIF4. *Current Biology* **19**(5): 408-413.

696 **Kolmos E, Nowak M, Werner M, Fischer K, Schwarz G, Mathews S, Schoof H, Nagy F,**
697 **Bujnicki JM, Davis SJ. 2009.** Integrating ELF4 into the circadian system through
698 combined structural and functional studies. *HFSP Journal* **3**(5): 350-366.

699 **Kuno N, Moller SG, Shinomura T, Xu XM, Chua NH, Furuya M. 2003.** The novel MYB
700 protein EARLY-PHYTOCHROME-RESPONSIVE1 is a component of a slave
701 circadian oscillator in Arabidopsis. *Plant Cell* **15**(10): 2476-2488.

702 **Legris M, Klose C, Burgie ES, Rojas CC, Neme M, Hiltbrunner A, Wigge PA, Schafer E,**
703 **Vierstra RD, Casal JJ. 2016.** Phytochrome B integrates light and temperature
704 signals in Arabidopsis. *Science* **354**(6314): 897-900.

705 **Lesk C, Rowhani P, Ramankutty N. 2016.** Influence of extreme weather disasters on
706 global crop production. *Nature* **529**(7584): 84-87.

707 **Li G, Siddiqui H, Teng YB, Lin RC, Wan XY, Li JG, Lau OS, Ouyang XH, Dai MQ, Wan JM,**
708 **et al. 2011.** Coordinated transcriptional regulation underlying the circadian
709 clock in Arabidopsis. *Nature Cell Biology* **13**(5): 616-622.

710 **Lin JY, Xu Y, Zhu ZQ. 2020.** Emerging plant thermosensors: from RNA to protein.
711 *Trends in Plant Science* **25**(12): 1187-1189.

712 **Lin LL, Little JW. 1989.** Autodigestion and reca-dependent cleavage of ind- mutant
713 LexA proteins. *Journal of Molecular Biology* **210**(3): 439-452.

714 **Marshall CM, Tartaglio V, Duarte M, Harmon FG. 2016.** The Arabidopsis sickle mutant
715 exhibits altered circadian clock responses to cool temperatures and
716 temperature-dependent alternative splicing. *Plant Cell* **28**(10): 2560-2575.

717 **Miura K, Jin JB, Hasegawa PM. 2007.** Sumoylation, a post-translational regulatory-
718 process in plants. *Current Opinion in Plant Biology* **10**(5): 495-502.

719 **Mizoguchi T, Wheatley K, Hanzawa Y, Wright L, Mizoguchi M, Song HR, Carre IA,**
720 **Coupland G. 2002.** LHY and CCA1 are partially redundant genes required to
721 maintain circadian rhythms in Arabidopsis. *Developmental Cell* **2**(5): 629-641.

722 **Mizuno T, Nomoto Y, Oka H, Kitayama M, Takeuchi A, Tsubouchi M, Yamashino T.**
723 **2014.** Ambient temperature signal feeds into the circadian clock
724 transcriptional circuitry through the EC night-time repressor in *Arabidopsis*
725 *thaliana*. *Plant and Cell Physiology* **55**(5): 958-976.

726 **Nagel DH, Doherty CJ, Pruneda-Paz JL, Schmitz RJ, Ecker JR, Kay SA. 2015.** Genome-
727 wide identification of CCA1 targets uncovers an expanded clock network in
728 Arabidopsis. *Proceedings of the National Academy of Sciences of the United*
729 *States of America* **112**(34): E4802-E4810.

730 **Nieto C, Lopez-Salmeron V, Daviere J-M, Prat S. 2015.** ELF3-PIF4 interaction regulates
731 plant growth independently of the Evening Complex. *Current Biology* **25**(2):
732 187-193.

733 **Nomoto Y, Kubozono S, Yamashino T, Nakamichi N, Mizuno T. 2012.** Circadian clock-
734 and PIF4-controlled plant growth: A coincidence mechanism directly integrates
735 a hormone signaling network into the photoperiodic control of plant
736 architectures in *Arabidopsis thaliana*. *Plant and Cell Physiology* **53**(11): 1950-
737 1964.

738 **Nusinow DA, Helfer A, Hamilton EE, King JJ, Imaizumi T, Schultz TF, Farre EM, Kay SA.**
739 **2011.** The ELF4-ELF3-LUX complex links the circadian clock to diurnal control
740 of hypocotyl growth. *Nature* **475**(7356): 398-402.

741 **Park YJ, Kim JY, Lee JH, Han SH, Park CM. 2021.** External and internal reshaping of
742 plant thermomorphogenesis. *Trends in Plant Science* **26**, 810-821.

743 **Quint M, Delker C, Franklin KA, Wigge PA, Halliday KJ, van Zanten M. 2016.** Molecular
744 and genetic control of plant thermomorphogenesis. *Nature Plants* **2**(1): 15190.

745 **Rawat R, Schwartz J, Jones MA, Sairanen I, Cheng Y, Andersson CR, Zhao Y, Ljung K,**
746 **Harmer SL. 2009.** REVEILLE1, a Myb-like transcription factor, integrates the
747 circadian clock and auxin pathways. *Proceedings of the National Academy of*
748 *Sciences of the United States of America* **106**(39): 16883-16888.

749 **Rawat R, Takahashi N, Hsu PY, Jones MA, Schwartz J, Salemi MR, Phinney BS, Harmer**
750 **SL. 2011.** REVEILLE8 and PSEUDO-RESPONSE REGULATOR5 form a negative
751 feedback loop within the *Arabidopsis* circadian clock. *PLoS Genetics* **7**(3),
752 e1001350.

753 **Rugnone ML, Soverna AF, Sanchez SE, Schlaen RG, Hernando CE, Seymour DK,**
754 **Mancini E, Chernomoretz A, Weigel D, Mac P, et al. 2013.** LNK genes integrate
755 light and clock signaling networks at the core of the *Arabidopsis* oscillator.
756 *Proceedings of the National Academy of Sciences of the United States of*
757 *America* **110**(29): 12120-12125.

758 **Shalit-Kaneh A, Kumimoto RW, Filkov V, Harmer SL. 2018.** Multiple feedback loops
759 of the *Arabidopsis* circadian clock provide rhythmic robustness across
760 environmental conditions. *Proceedings of the National Academy of Sciences of*
761 *the United States of America* **115**(27): 7147-7152.

762 **Silva CS, Nayak A, Lai X, Hutin S, Hugouvieux V, Jung J-H, Lopez-Vidriero I, Franco-**
763 **Zorrilla JM, Panigrahi KCS, Nanao MH, et al. 2020.** Molecular mechanisms of
764 Evening Complex activity in *Arabidopsis*. *Proceedings of the National Academy*
765 *of Sciences of the United States of America* **117**(12): 6901-6909.

766 **Song ZT, Sun L, Lu SJ, Tian Y, Ding Y, Liu JX. 2015.** Transcription factor interaction with
767 COMPASS-like complex regulates histone H3K4 trimethylation for specific gene
768 expression in plants. *Proceedings of the National Academy of Sciences of the*
769 *United States of America* **112**(9): 2900-2905.

770 **Sun J, Qi L, Li Y, Chu J, Li C. 2012.** PIF4-mediated activation of *YUCCA8* expression
771 integrates temperature into the auxin pathway in regulating Arabidopsis
772 hypocotyl growth. *PLoS Genetics* **8**(3), e1002594.

773 **Thines B, Harmon FG. 2010.** Ambient temperature response establishes ELF3 as a
774 required component of the core Arabidopsis circadian clock. *Proceedings of*
775 *the National Academy of Sciences of the United States of America* **107**(7): 3257-
776 3262.

777 **Vu LD, Xu X, Gevaert K, Smet I. 2019.** Developmental plasticity at high temperature.
778 *Plant Physiology* **181**(2): 399-411.

779 **Wang S, Ding L, Liu JX, Han JJ. 2018.** PIF4-regulated thermo-responsive genes in
780 Arabidopsis. *Biotechnology Bulletin* **34**(7): 57-65.

781 **Wang ZY, Tobin EM. 1998.** Constitutive expression of the *CIRCADIAN CLOCK*
782 *ASSOCIATED 1 (CCA1)* gene disrupts circadian rhythms and suppresses its own
783 expression. *Cell* **93**(7): 1207-1217.

784 **Xie QG, Wang P, Liu X, Yuan L, Wang LB, Zhang CG, Li Y, Xing HY, Zhi LY, Yue ZL, et al.**
785 **2014.** LNK1 and LNK2 are transcriptional coactivators in the Arabidopsis
786 circadian oscillator. *Plant Cell* **26**(7): 2843-2857.

787 **Zhang LL, Li W, Tian YY, Davis SJ, Liu JX. 2021.** The E3 ligase XBAT35 mediates
788 thermoresponsive hypocotyl growth by targeting ELF3 for degradation in
789 Arabidopsis. *Journal of Integrative Plant Biology* **63**, 1097-1103.

790 **Zhang LL, Luo A, Davis SJ, Liu JX. 2021a.** Timing to grow: roles of clock in
791 thermomorphogenesis. *Trends in Plant Science* **26**(12), 1248-1257.

792 **Zhang LL, Shao YJ, Ding L, Wang MJ, Davis SJ, Liu JX. 2021b.** XBAT31 regulates
793 thermoresponsive hypocotyl growth through mediating degradation of the
794 thermosensor ELF3 in Arabidopsis. *Science Advances* **7**(19), eabf4427.

795 **Zhang SS, Yang H, Ding L, Song ZT, Ma H, Chang F, Liu JX. 2017.** Tissue-specific
796 transcriptomics reveals an important role of the unfolded protein response in
797 maintaining fertility upon heat stress in Arabidopsis. *Plant Cell* **29**(5): 1007-
798 1023.

799 **Zhu JY, Oh E, Wang T, Wang ZY. 2016.** TOC1-PIF4 interaction mediates the circadian
800 gating of thermoresponsive growth in Arabidopsis. *Nature Communications* **7**:
801 13692.

802

803

804

805 **FIGURE LEGENDS**

806 **Fig. 1. RVE5 inhibits hypocotyl growth at warm temperatures and**
807 **functions upstream of *PIF4* in *Arabidopsis*.**

808 **(a-b)**, Phenotypes of *RVE5* loss-of-function mutant and genetic complemented
809 plants. Seedlings of wild-type (WT) plants, *RVE5* mutant (*rve5-2*), and genetic
810 complemented plants (COM25/COM34/COM29) were examined for phenotypic
811 analysis. **(c-d)**, Genetic analysis of *RVE5* and *PIF4* in thermo-responsive
812 hypocotyl growth. The WT, *pif4-101* and *rve5-2* single mutants, and *rve5-2 pif4-*
813 *101* double mutant plants were checked for phenotypes. All the materials grown
814 at 22°C were kept at 22°C or transferred to 29°C for 4 days (a-b) or 3 days (c-
815 d), after which plants were imaged and their hypocotyl lengths were
816 subsequently measured. Error bars depict *SD* (n=22). Letters above the bars
817 indicate significant differences as determined by HSD test ($P < 0.05$). Bar = 5
818 mm.

819 **Fig. 2. RVE5 has overlapping genome-wide direct targets including clock-**
820 **associated genes with CCA1.**

821 **(a)**, Accumulation of RVE5 protein level in response to warm temperature.
822 Seven-day-old *RVE5-MYC* transgenic seedlings grown at 22°C were kept at
823 22°C or transferred to 29°C, after which the fusion protein was checked by
824 western blotting with *anti-MYC* antibody. Tubulin served as a protein loading
825 control. Signal intensity of each band was quantified and normalized to that of
826 the first sample. **(b-d)**, ChIP-Seq analysis of RVE5-binding targets. The
827 distribution of ChIP-Seq signals on genebody, upstream 2K and downstream
828 2K regions was examined (b) and the common RVE5-binding motifs among the
829 385 binding peaks were obtained (c-d). **(e)**, Venn diagram showing the number
830 of overlapping binding targets between RVE5 and CCA1. **(f)**, Distribution of
831 RVE5-binding peaks on clock-related genes in the Integrative Genomics
832 Viewer. In the gene model, blue boxes represent exons and blue lines represent

833 introns, arrows indicate the direction of transcription. Reads are aligned from
834 input (blue) and ChIP (red) with three replicates. Binding to the promoter of
835 *ELF3*, *PRR9*, *CCA1*, *LHY*, or *PIF4* was not significant ($P < 0.05$). **(g-i)**, *in vivo*
836 binding of RVE5 to the promoters of *ELF4*, *PRR5* and *PRR7* under two
837 temperature conditions. Transgenic plants overexpressing *RVE5-MYC* grown
838 at 22°C or 29°C for 12 hr or 36 hr were harvested and ChIP-qPCR was
839 performed using *anti-MYC* antibody. Relative enrichment of each sample was
840 normalized to that *anti-GST* sample (IgG control) in 12 hr at 22°C, both of which
841 were normalized to that of the *TA3* control. Error bar represents SE ($n = 3$).
842 Letters above the bars indicate significant differences as determined by HSD
843 test ($P < 0.05$).

844 **Fig. 3. RVE5 regulates the expression of clock-associated genes under**
845 **warm temperature conditions.**

846 Five-day-old WT plants as well as *RVE5* mutant (*rve5-2*) plants grown at 22°C
847 were kept at 22°C or transferred to 29°C, after which total seedlings were
848 sampled at different ZT times as indicated for RT-qPCR analysis. Relative gene
849 expression is the expression level of each gene normalized to that of *PP2A*.
850 The bars depict the *SE* ($n=3$).

851 **Fig. 4. RVE5 has a weaker transcriptional repression activity than CCA1.**
852 **(a-b)**, Direct binding of RVE5 or CCA1 to the *ELF4* promoter sequence. MBP-
853 tagged RVE5 (a) or CCA1 (b) was incubated with the biotin-labelled *ELF4*
854 promoter DNA (5'-AAATATCT-3'). Non-labelled native (competitor) or mutated
855 (5'-AAATCGAG-3') cold probes [competitor (m)] were used in the competing
856 assays. **(c)**, Transcriptional activation activity assay in yeast cells. RVE5 was
857 fused to the yeast GAL4 DNA-binding domain (BD). Activation of the His and
858 Ade reporter genes in yeast cells was used for the activation assay.
859 CONSTANS (CO) was used as a positive control. **(d-g)**, Transcriptional
860 repression activity assay in effector-reporter assays. Schematic design for the

861 assay is shown in d. LexA-RVE5 or LexA-CCA1 (e), or RVE5 and CCA1 (f-g)
862 driven by the CaMV 35S promoter was expressed as the effector, and the
863 CaMV 35S constitutive promoter linked with a promoter-specific sequence of
864 either pLexA or pELF4 to the firefly luciferase was used as a reporter. Renilla
865 luciferase driven by the CaMV 35S promoter was used as an internal control.
866 Relative luciferase activity is the firefly luciferase activity normalized to the
867 Renilla luciferase activity, which was then normalized to the empty vector
868 control. Western blots showing the expression level of the effector (RVE5-
869 MYC/CCA1-MYC) in the effector-reporter assays in tobacco leaves (g). RbcS
870 serves as a loading control. Error bars depict *SE* (n=5 in e, n=7 in f). Letters
871 above the bars indicate significant differences as determined by HSD test ($P <$
872 0.05).

873 **Fig. 5. RVE5 competes with CCA1 in DNA-binding under warm**
874 **temperature conditions.**

875 **(a-d)**, Accumulation of CCA1 protein at warm temperatures. *CCA1-FLAG* was
876 expressed with the *CCA1* native promoter in the wild-type (WT) or *rve5-2*
877 mutant background. The fusion protein in the WT background (*CCA1-21*, a) and
878 *rve5-2* mutant background (*CCA1-17*, b) were checked with *anti-FLAG*
879 antibody at different time under two temperature conditions. Tubulin served as
880 a protein loading control. Signal intensity of each band was quantified and
881 normalized to that of the first sample (a-b). Two sets of independent lines with
882 comparable expression level in WT (*CCA1-21/26*) and *rve5-2* mutant (*CCA1-*
883 *17/13*) backgrounds were selected, and the fusion proteins were checked in the
884 same blot by Western blotting at ZT 12 hr (c-d). Three independent blots were
885 run and quantified for each set of comparison (c-d). **(e-f)**, Direct binding of
886 CCA1 to the *ELF4* promoter in WT and *rve5-2* mutant plants. Transgenic plants
887 expressing *CCA1-FLAG* in WT background and *rve5-2* mutant background
888 grown at 29°C were harvested at ZT 12 hr for ChIP-qPCR using *anti-FLAG*

889 antibody. IgG was used as a negative control. Relative enrichment of each
890 sample was normalized to that of IgG sample at 29°C, both of which were
891 normalized to that of the *TA3* control. Error bar represents SE (n = 3).

892 **Fig. 6. RVE5 and CCA1/LHY have competitive roles in thermoresponsive**
893 **hypocotyl regulation.**

894 **(a-d)**, Regulation of *ELF4* and *PIF4* expression in *CCA1-FLAG* expressing
895 plants in the wild-type (WT) or *rve5-2* mutant background driven by the *CCA1*
896 native promoter at ZT 36 hr. Relative gene expression is the expression level
897 of *ELF4* or *PIF4* normalized to that of *PP2A*. The bars depict the SE (n=3). **(e-**
898 **h)**, Genetic analysis of *RVE5* and *CCA1/LHY* in thermomorphogenesis. The
899 WT, *rve5-2*, *cca1-1*, *rve5-2 cca1-1*, *rve5-2 lhy-20*, and *rve5-2 cca1-1 lhy-20*
900 plants were phenotyped. Error bars depict SD (n=30). Letters above the bars
901 indicate significant differences as determined by HSD test ($P < 0.05$); Bar = 5
902 mm.

903 **Fig. 7. Overexpression of ELF4 rescues the thermoresponsive hypocotyl**
904 **phenotype of rve5-2 mutant plants.**

905 **(a-d)**, Suppression of *rve5-2* mutant phenotype under warm temperature
906 conditions by overexpression of *ELF4*. *ELF4* was overexpressed in the WT
907 (*ELF4ox*) and *rve5-2* mutant (*rve5-2 ELF4ox*) background and two independent
908 transgenic lines in each background with similar transgene expression levels
909 selected and phenotyped (a-b). The expression of total *ELF4* and *PIF4* was
910 checked by RT-qPCR at ZT 36 hr (c-d). Relative gene expression is the
911 expression level in each sample normalized to that of *PP2A*. The bars depict
912 the SE (n=3). **(e-g)**, Genetic analysis between *RVE5* and *ELF4*. The *rve5-2*
913 single mutant and *elf4-209* single mutant were crossed to generate the double
914 mutant *rve5-2 elf4-209*, and the single and double mutants were phenotyped
915 (e-f). The expression of *PIF4* was checked by RT-qPCR (g). All the materials
916 grown at 22°C were kept at 22°C or transferred to 29°C for 4 days, after which

917 plants were imaged and their hypocotyl lengths were subsequently measured.
918 Error bars depict SD (n=30). Letters above the bars indicate significant
919 differences as determined by HSD test ($P < 0.05$). Bar = 5 mm.

920 **Fig. 8. A competition-attenuation working model for modulating *ELF4***
921 **expression and thermoresponsive hypocotyl growth.**

922 In WT plants, both RVE5 and CCA1 are transcriptional repressors and bind to
923 the same *cis*-element presented on *ELF4* promoter. CCA1 has a stronger (S)
924 while RVE5 has a weaker (W) transcriptional repression activity. Therefore,
925 RVE5 attenuates the repression effect of CCA1 through competing with CCA1
926 in DNA binding and maintains the expression of downstream genes including
927 *ELF4* at warm temperatures. The encoded ELF4 is assembled into an evening
928 complex (EC) together with ELF3 and LUX to inhibit the expression of *PIF4*, a
929 central regulator of thermomorphogenesis. In *rve5-2* mutant plants, due to the
930 absence of RVE5, more CCA1 binds to the *ELF4* promoter and results in more
931 inhibition of *ELF4* expression, leading to more *PIF4* expression, and
932 subsequent more hypocotyl growth under warm temperature conditions.

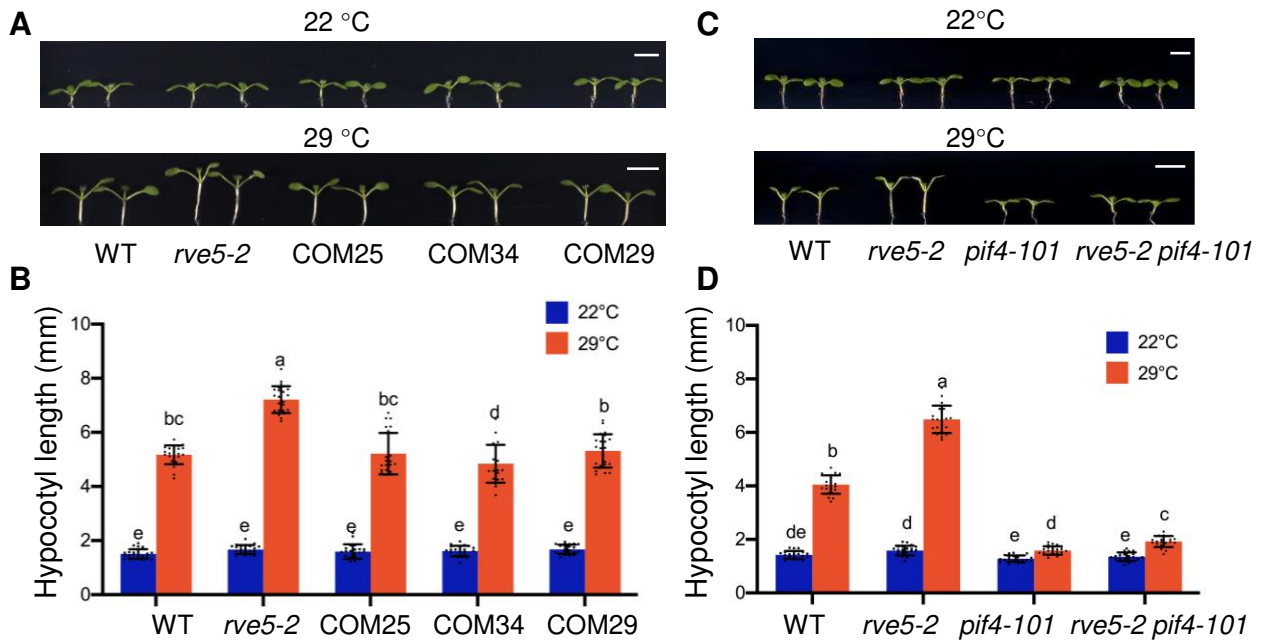


Figure 1. RVE5 Inhibits Hypocotyl Growth at Warm Temperatures and Functions Upstream of PIF4 in Arabidopsis.

A-B, Phenotypes of *RVE5* loss-of-function mutant and genetic complemented plants. Seedlings of wild-type (WT) plants, *RVE5* mutant (*rve5-2*), and genetic complemented plants (COM25/COM34/COM29) were examined for phenotypic analysis. **C-D,** Genetic analysis of *RVE5* and *PIF4* in thermo-responsive hypocotyl growth. The WT, *pif4-101* and *rve5-2* single mutants, and *rve5-2 pif4-101* double mutant plants were checked for phenotypes. All the materials grown at 22° C were kept at 22° C or transferred to 29° C for 4 days, after which plants were imaged and their hypocotyl lengths were subsequently measured. Error bars depict SD (n=22). Letters above the bars indicate significant differences as determined by HSD test (P < 0.05). Bar = 5 mm.

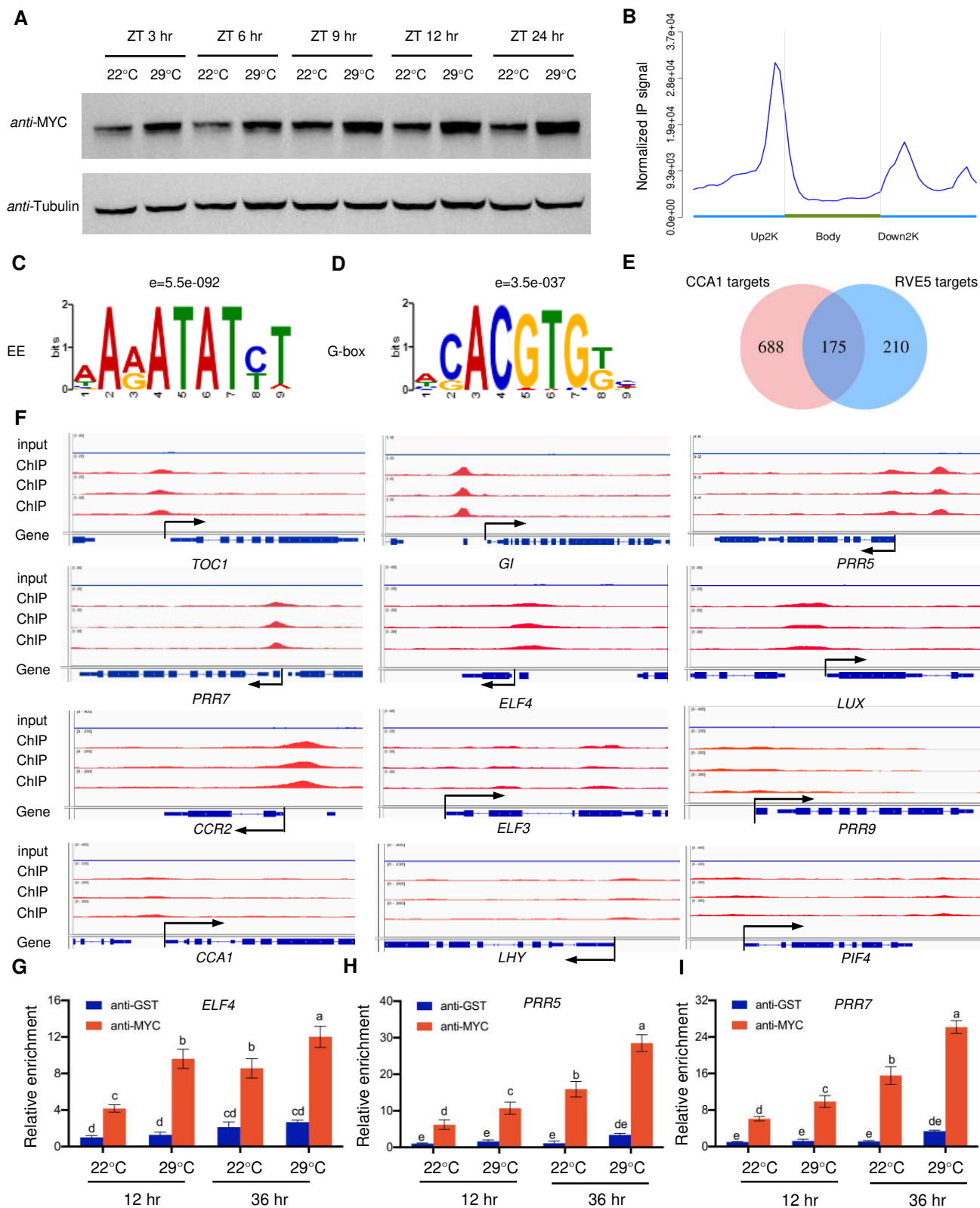


Figure 2. RVE5 Has Overlapping Genome-Wide Direct Targets including Clock-Associated Genes with CCA1.

A, Accumulation of RVE5 protein level in response to warm temperature. Seven-day-old *RVE5-MYC* transgenic seedlings grown at 22°C were kept at 22°C or transferred to 29°C, after which the fusion protein was checked by western blotting with *anti-MYC* antibody. Tubulin served as a protein loading control. **B-D**, ChIP-Seq analysis of RVE5-binding targets. The distribution of ChIP-Seq signals on genebody, upstream 2K and downstream 2K regions was examined (B) and the common RVE5-binding motifs among the 385 binding peaks were obtained (C-D). **E**, Venn diagram showing the number of overlapping binding targets between RVE5 and CCA1. **F**, Distribution of RVE5-binding peaks on clock-related genes in the Integrative Genomics Viewer. In the gene model, blue boxes represent exons and blue lines represent introns, arrows indicate the direction of transcription. Reads are aligned from input (blue) and ChIP (red) with three replicates. Binding to the promoter of *ELF3*, *PRR9*, *CCA1*, *LHY*, or *PIF4* was not significant ($P < 0.05$). **G-I**, *in vivo* binding of RVE5 to the promoters of *ELF4*, *PRR5* and *PRR7* under two temperature conditions. Transgenic plants overexpressing *RVE5-MYC* grown at 22°C or 29°C for 12 hr or 36 hr were harvested and ChIP-qPCR was performed using anti-MYC antibody. Relative enrichment of each sample was normalized to that anti-GST sample (IgG control) in 12 hr at 22°C, both of which were normalized to that of the *TA3* control. Error bar represents SE ($n = 3$). Letters above the bars indicate significant differences as determined by HSD test ($P < 0.05$).

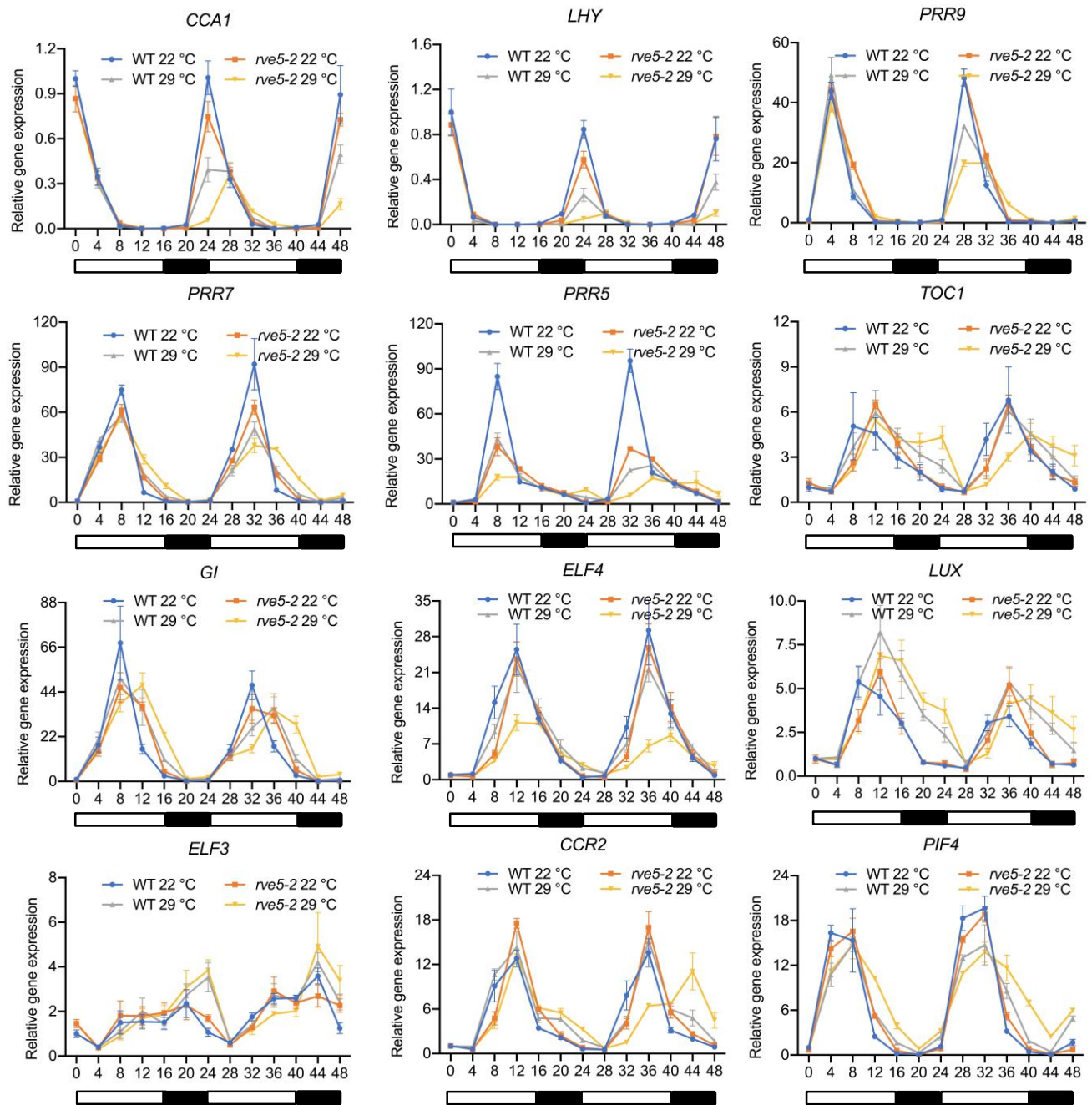


Figure 3. RVE5 Regulates the Expression of Clock-Associated Genes under Warm Temperature Conditions.

Expression of clock-associated genes in WT and *rve5-2* mutant plants under warm temperature conditions. Five-day-old WT plants as well as *RVE5* mutant (*rve5-2*) plants grown at 22 °C were kept at 22 °C or transferred to 29 °C, after which total seedlings were sampled at different ZT times as indicated for RT-qPCR analysis. Relative gene expression is the expression level of each gene normalized to that of *PP2A*. The bars depict the SE (n=3).

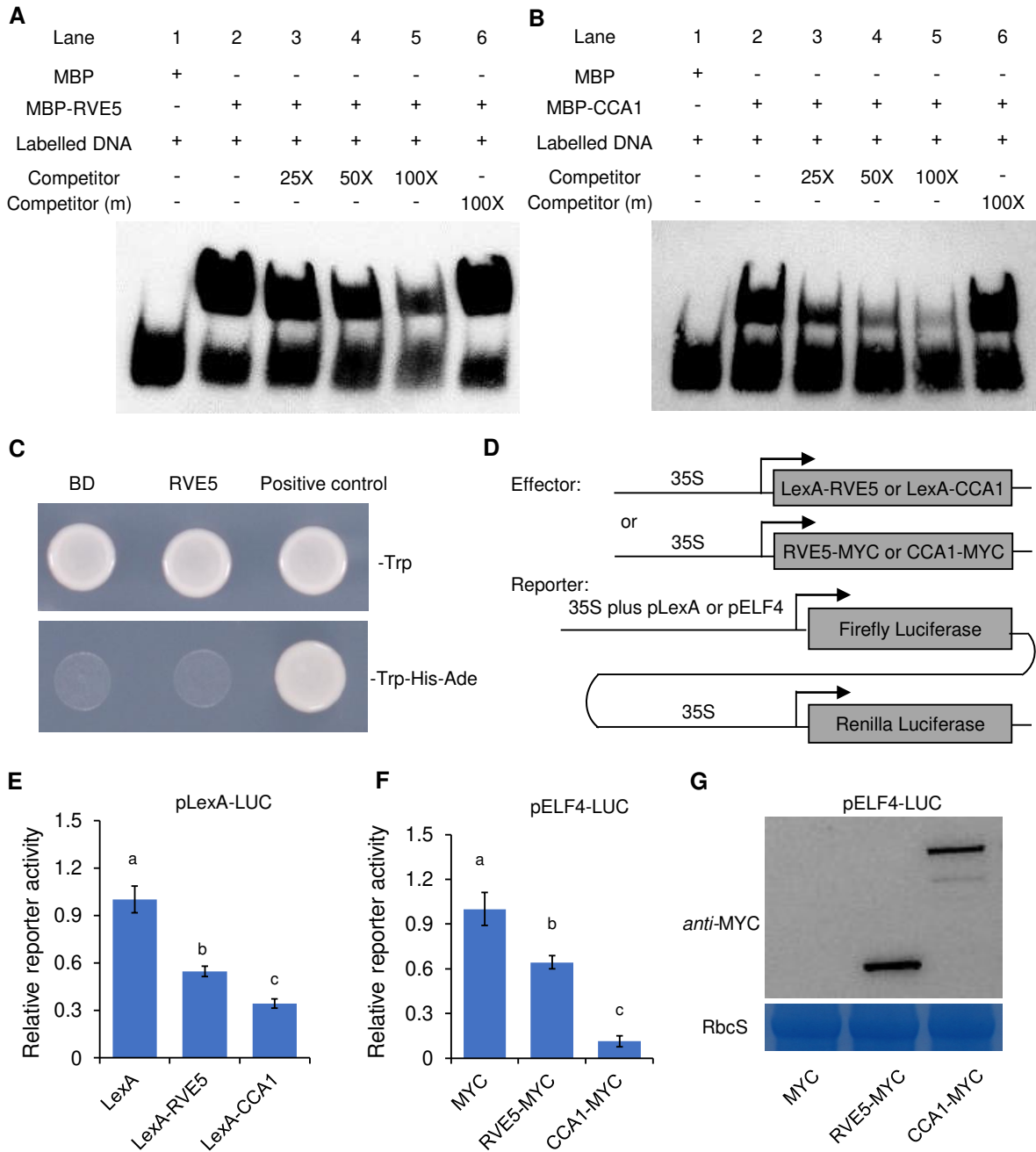


Figure 4. RVE5 Has a Weaker Transcriptional Repression Activity than CCA1.

A-B, Direct binding of RVE5 or CCA1 to the *ELF4* promoter sequence. MBP-tagged RVE5 (A) or CCA1 (B) was incubated with the biotin-labelled *ELF4* promoter DNA. Non-labelled cold probes (native or mutated competitor) were used in the competing assays. **C**, Transcriptional activation activity assay in yeast cells. RVE5 was fused to the yeast GAL4 DNA-binding domain (BD). Activation of the His and Ade reporter genes in yeast cells was used for the activation assay. CONSTANS (CO) was used as a positive control. **D-G**, Transcriptional repression activity assay in effector-reporter assays. Schematic design for the assay is shown in D. LexA-RVE5 or LexA-CCA1 (F), or RVE5 and CCA1 (G) driven by the CaMV 35S promoter was expressed as the effector, and the CaMV 35S constitutive promoter linked with a promoter-specific sequence of either pLexA or pELF4 to the firefly luciferase was used as a reporter. Renilla luciferase driven by the CaMV 35S promoter was used as an internal control. Relative luciferase activity is the firefly luciferase activity normalized to the Renilla luciferase activity, which was then normalized to the empty vector control. Western blots showing the expression level of the effector (RVE5-MYC/CCA1-MYC) in the effector-reporter assays in tobacco leaves (G). RbcS serves as a loading control. Error bars depict SE (n=5 in e, n=7 in f). Letters above the bars indicate significant differences as determined by HSD test (P < 0.05).

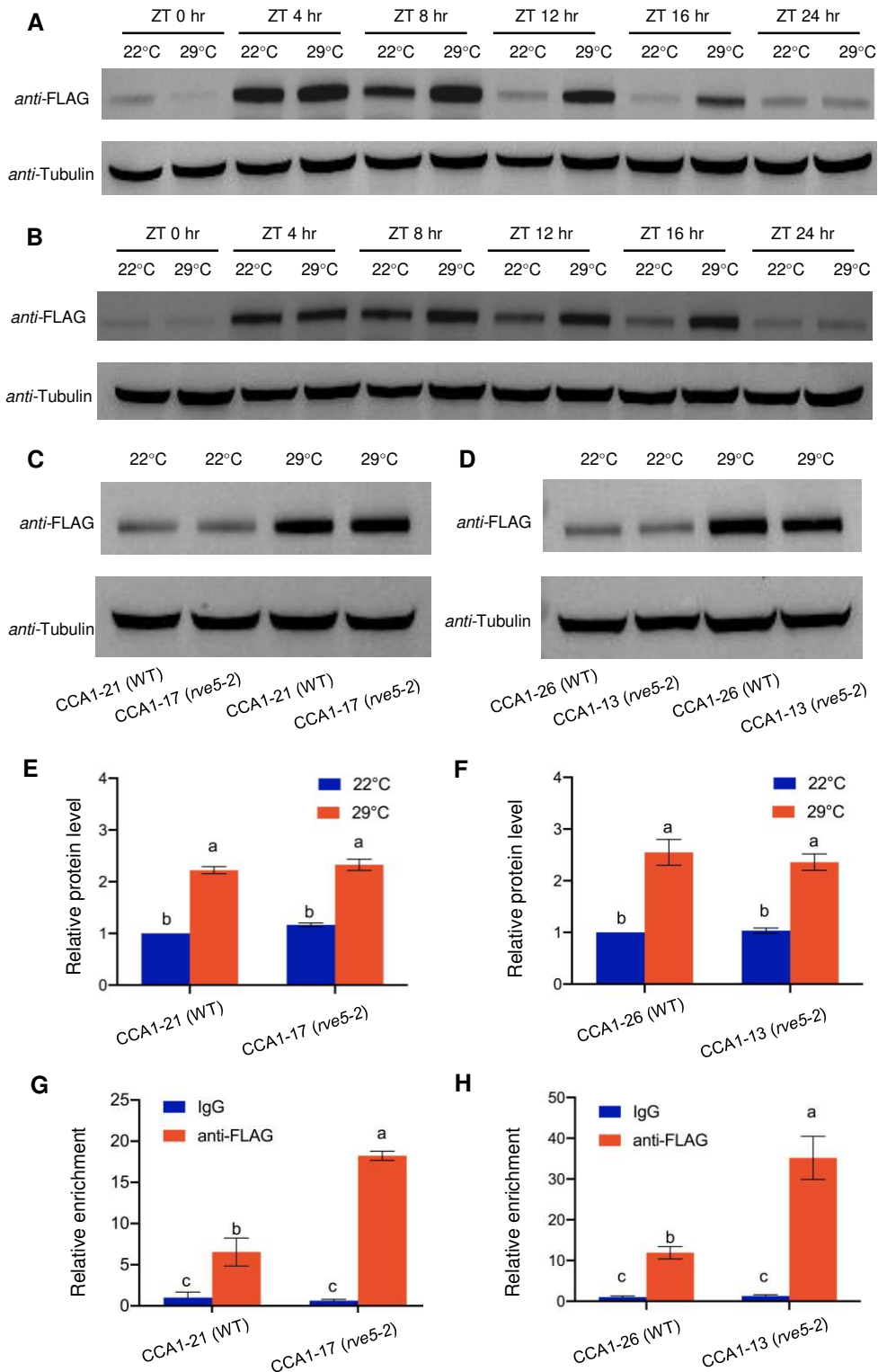


Figure 5. RVE5 Competes with CCA1 in DNA-Binding under Warm Temperature Conditions.

A-F, Accumulation of CCA1 protein at warm temperatures. *CCA1-FLAG* was expressed with the *CCA1* native promoter in the wild-type (WT) or *rve5-2* mutant background. The fusion protein in the WT background (CCA1-21) and *rve5-2* mutant background (CCA1-17) were checked with *anti-FLAG* antibody at different time under two temperature conditions (A-B). Two independent lines with comparable expression level in WT and backgrounds were selected, and the fusion protein was checked at ZT 12 hr (C-F). Tubulin served as a protein loading control. Three independent blots were quantified. **G-H**, Direct binding of CCA1 to the *ELF4* promoter in WT and *rve5-2* mutant plants. Transgenic plants expressing *CCA1-FLAG* in WT background and *rve5-2* mutant background grown at 29° C were harvested at ZT 12 hr for ChIP-qPCR using *anti-FLAG* antibody. IgG was used as a negative control. Relative enrichment of each sample was normalized to that of IgG sample at 29° C, both of which were normalized to that of the *TA3* control. Error bar represents SE (n = 3).

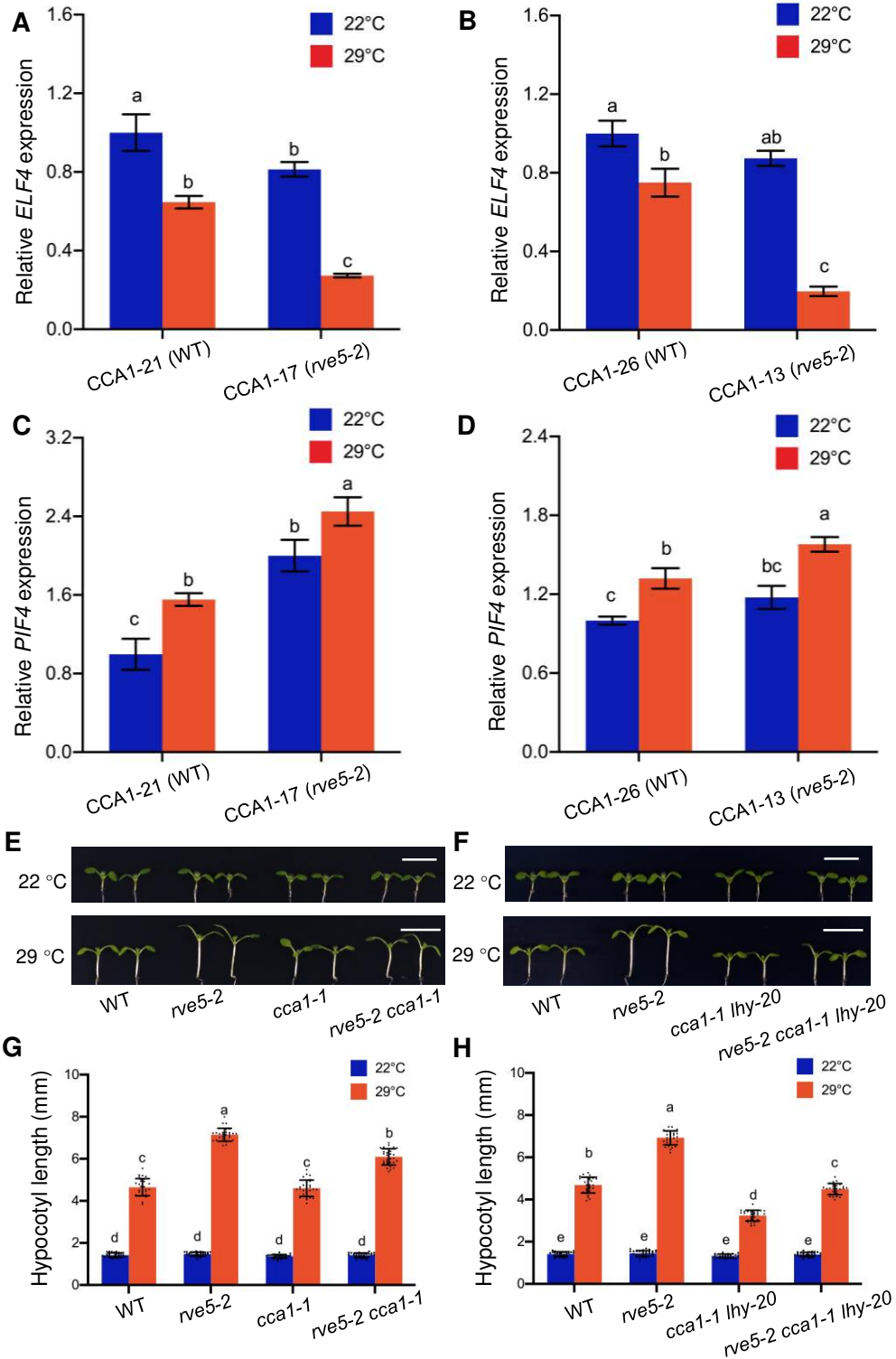


Figure 6. RVE5 and CCA1/LHY Have Competitive Roles in Thermoresponsive Hypocotyl Regulation.

A-D, Regulation of *ELF4* and *PIF4* expression in *CCA1-FLAG* expressing plants in the wild-type (WT) or *rve5-2* mutant background driven by the *CCA1* native promoter at ZT 36 hr. Relative gene expression is the expression level of *ELF4* or *PIF4* normalized to that of *PP2A*. The bars depict the *SE* ($n=3$). **E-H**, Genetic analysis of *RVE5* and *CCA1/LHY* in thermomorphogenesis. The WT, *rve5-2*, *cca1-1*, *rve5-2 cca1-1*, *rve5-2 lhy-20*, and *rve5-2 cca1-1 lhy-20* plants were phenotyped. Error bars depict *SD* ($n=30$). Letters above the bars indicate significant differences as determined by HSD test ($P < 0.05$); Bar = 5 mm.

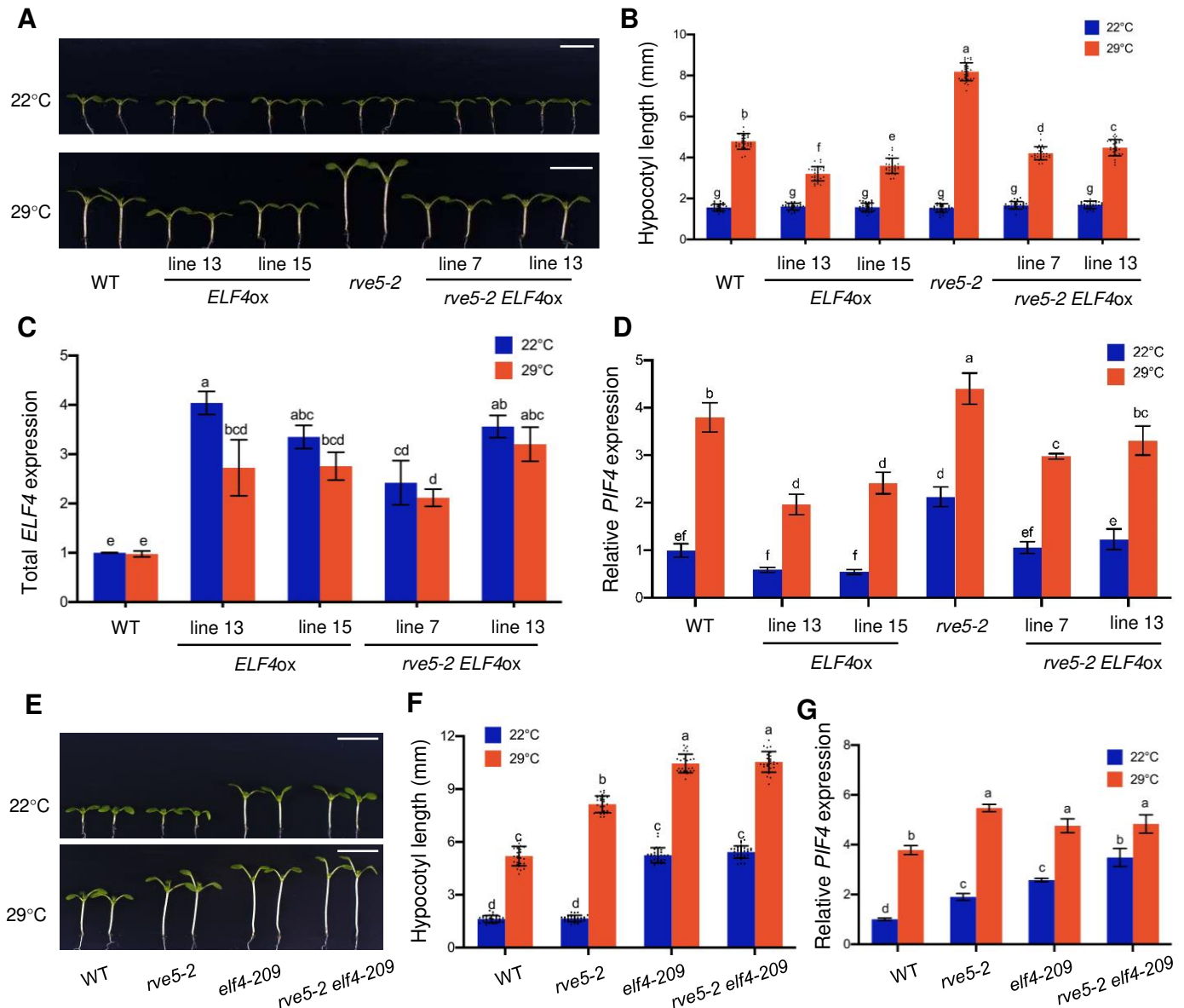


Figure 7. Overexpression of *ELF4* Rescues the Thermoresponsive Hypocotyl Phenotype of *rve5-2* Mutant Plants.

A-D, Suppression of *rve5-2* mutant phenotype under warm temperature conditions by overexpression of *ELF4*. *ELF4* was overexpressed in the WT (*ELF4ox*) and *rve5-2* mutant (*rve5-2 ELF4ox*) background and two independent transgenic lines in each background with similar transgene expression levels selected and phenotyped (A-B). The expression of total *ELF4* and *PIF4* was checked by RT-qPCR at ZT 36 hr (C-D). Relative gene expression is the expression level in each sample normalized to that of *PP2A*. The bars depict the SE (n=3). **E-G**, Genetic analysis between *RVE5* and *ELF4*. The *rve5-2* single mutant and *elf4-209* single mutant were crossed to generate the double mutant *rve5-2 elf4-209*, and the single and double mutants were phenotyped (E-F). The expression of *PIF4* was checked by RT-qPCR (G). All the materials grown at 22° C were kept at 22° C or transferred to 29° C for 4 days, after which plants were imaged and their hypocotyl lengths were subsequently measured. Error bars depict SD (n=30). Letters above the bars indicate significant differences as determined by HSD test (P < 0.05). Bar = 5 mm.

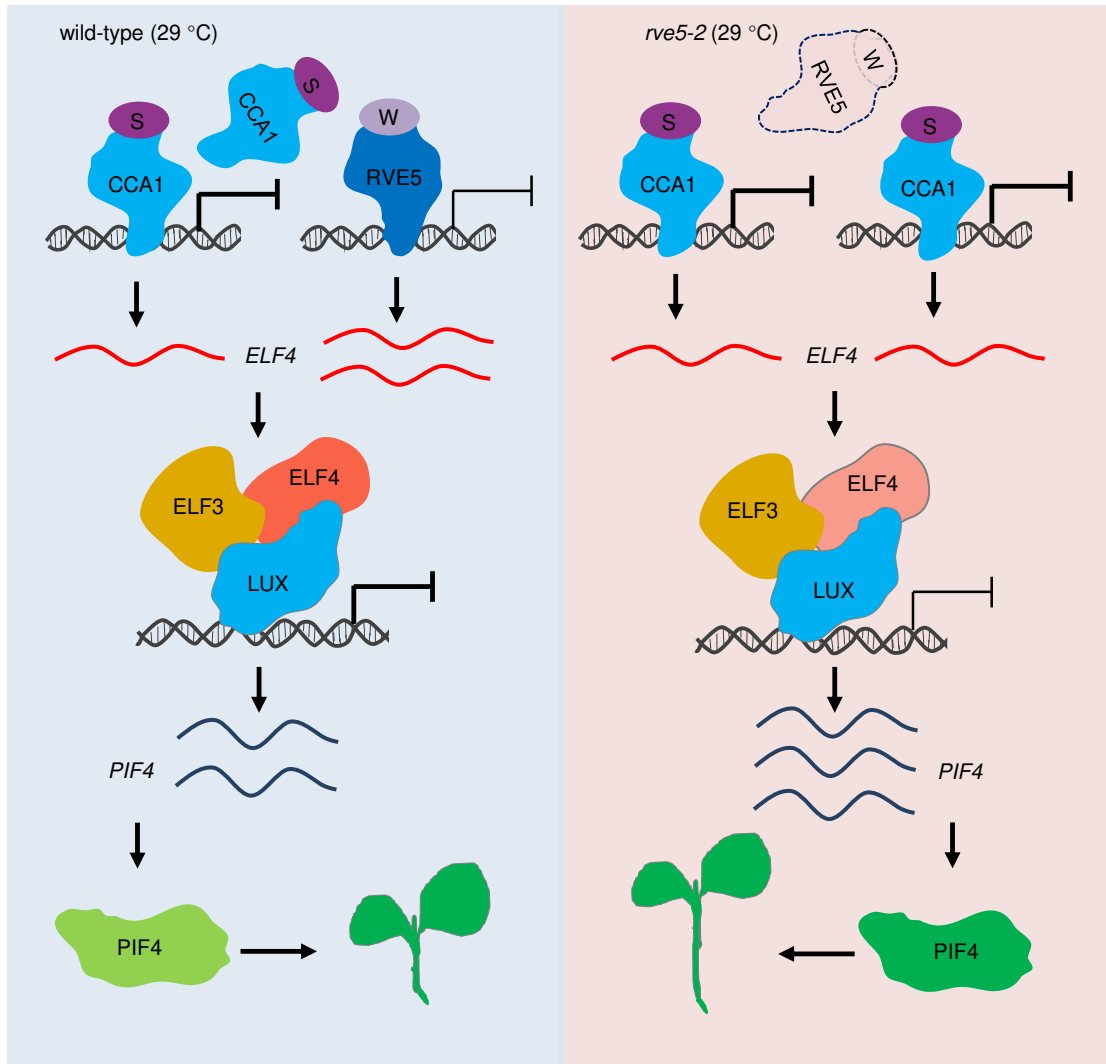


Figure 8. A competition-attenuation working model for modulating *ELF4* expression and thermoresponsive hypocotyl growth.

In WT plants, both RVE5 and CCA1 are transcriptional repressors and bind to the same *cis*-element presented on *ELF4*. CCA1 has a stronger (S) while RVE5 has a weaker (W) transcriptional repression activity. Therefore, RVE5 attenuates the repression effect of CCA1 through competing with CCA1 in DNA binding and maintains the expression of downstream genes including *ELF4* at warm temperatures. The encoded ELF4 is assembled into an evening complex (EC) together with ELF3 and LUX to inhibit the expression of *PIF4*, a central regulator of thermomorphogenesis. In *rve5-2* mutant plants, due to the absence of RVE5, more CCA1 binds to the *ELF4* promoter and results in more inhibition of *ELF4* expression, leading to disinhibition and more *PIF4* expression, and subsequent more hypocotyl growth under warm temperature conditions.